

3 The Precambrian paleogeography of Laurentia

Nicholas L. Swanson-Hysell¹

¹ Department of Earth and Planetary Science, University of California, Berkeley, CA 94720 USA

This chapter is in preparation for the book Ancient Supercontinents and the Paleogeography of the Earth

¹ 3.1 Abstract

Laurentia was a major continent throughout the majority of the Proterozoic. It is hypothesized to have had a central position in both the Paleoproterozoic Nuna and Neoproterozoic Rodinia supercontinents. The paleogeographic position of Laurentia is key to the development of reconstructions of Proterozoic paleogeography. There is a rich record of Precambrian paleomagnetic poles from Laurentia, as well as an extensive and well-documented geologic history of tectonism. These geologic and paleomagnetic records are increasingly better constrained geochronologically and are both key to evaluating and developing paleogeographic models. Data from the Slave and Superior provinces of Laurentia provide what is arguably the strongest evidence of differential plate tectonics in the Rhyacian and Orosirian Periods of the Paleoproterozoic Era (2.3 to 1.8 Ga) leading up to the collision of these terranes during the Trans-Hudson orogeny. The collisions of these and other Archean provinces led to the formation of the core of Laurentia. Subsequent crustal growth occurred through multiple intervals of accretionary orogenesis through the late Paleoproterozoic and Mesoproterozoic until the continent-continent collision of the Grenvillian orogeny that was ongoing at the Mesoproterozoic-Neoproterozoic boundary (1.0 Ga). The lead-up to this orogeny was associated with rapid plate motion of Laurentia from high latitudes towards the equator recorded by the Logan Loop and Keweenawan Track of paleomagnetic poles. Following, a return to high-latitudes as constrained by paleomagnetic poles of the Grenville Loop, Laurentia straddled the equator at the time of Cryogenian Snowball Earth glaciation as part of the Rodinia supercontinent. Rifting and passive margin development then isolated Laurentia in the early Paleozoic Era. Subsequent

22 accretionary and collisional orogenesis occurred associated with the Appalachian orogenic cycle
23 with Laurentia first colliding with Avalonia- Baltica to become Laurussia and Laurussia then
24 uniting with Gondwana to form Pangea. While the details of the conjugate continents are better
25 reconstructed for this last Wilson cycle, the broad features of the Trans-Hudson, Grenvillian and
26 Appalachian orogenic cycles bear similarities. In each case, accretionary collision of arc terranes
27 was followed by continent-continent collision. The major difference is that the collisions of the
28 Grenvillian and Appalachian orogenic cycles resulted in relatively minor crustal growth compared
29 to the Trans-Hudson. Break-up following the Grenvillian and Appalachian orogenic cycles
30 occurred along the same margin as collision while the major orogens of the Trans-Hudson
31 orogenic cycle have remained sutured. As a result, Laurentia has been a formidable continent for
32 the past 1.8 billion years whose position and history is key for reconstructing global
33 paleogeography. The evidence from Laurentia provides strong-support for mobile lid plate
34 tectonic processes operating over the past 2.2 billion years.

35 **3.2 Introduction and broad tectonic history**

36 Laurentia refers to the craton that forms the Precambrian core of North America (Fig. 1).
37 Laurentia is comprised of multiple Archean provinces that had unique histories prior to their
38 amalgamation in the Paleoproterozoic, as well as tectonic zones of crustal growth that post-date
39 this assembly (Hoffman, 1989; Whitmeyer and Karlstrom, 2007). Collision between the Superior
40 province and the composite Slave+Rae+Hearne provinces that resulted in the Trans-Hudson
41 orogeny represents a major event in the formation of Laurentia (Corrigan et al., 2009). Terminal
42 collision recorded in the Trans-Hudson orogen is estimated to have been ca. 1.86 to 1.82 Ga based
43 on constraints such as U-Pb dating of monazite grains and zircon rims (Skipton et al., 2016;
44 Weller and St-Onge, 2017, e.g.). A period of accretionary and collision orogenesis is recorded in
45 the constituent provinces and terranes of Laurentia leading up to the terminal collision of the
46 Trans-Hudson orogeny. This overall story of rapid Paleoproterozoic amalgamation of Laurentia's
47 constituent Archean provinces, including the terminal Trans-Hudson orogeny, was synthesized in
48 the seminal *United Plates of America* paper of Hoffman (1988) and has been refined in the time
49 since – particularly with additional geochronological constraints. Of most relevance here are the

50 events that led to the suturing of more major Archean provinces: the Thelon orogen associated
51 with the collision between the Slave and Rae provinces ca. 2.0 to 1.9 Ga (Hoffman, 1989); the
52 Snowbird orogen associated with ca. 1.89 Ga collision between the Rae and Hearne provinces and
53 associated terranes (Berman et al., 2007); the Nagssugtoqidian orogen due to the ca. 1.86 to 1.84
54 Ga collision between the Rae and North Atlantic provinces (St-Onge et al., 2009); and the
55 Torngat orogen resulting from the ca. 1.87 to 1.85 Ga collision of the Meta Incognita province
56 (grouped with the Rae province in older compilations) with the North Atlantic province (St-Onge
57 et al., 2009). As for the Wyoming province, many models posit that it was conjoined with Hearne
58 and associated provinces at the time of the Trans-Hudson orogeny (e.g. St-Onge et al., 2009;
59 Pehrsson et al., 2015) or was proximal to Hearne and Superior while still undergoing continued
60 translation up to ca. 1.80 Ga (Whitmeyer and Karlstrom, 2007). A contrasting view has been
61 proposed that the Wyoming province and Medicine Hat blocks were not conjoined with the
62 other Laurentia provinces until ca. 1.72 Ga (Kilian et al., 2016). This interpretation is argued to
63 be consistent with geochronological constraints on monazite and metamorphic zircon indicating
64 active collisional orogenesis associated with the Big Sky orogen on the northern margin of the
65 craton as late as ca. 1.75 to 1.72 Ga (Condit et al., 2015) and ca. 1.72 tectonomagmatic activity
66 in the Black Hills region (Redden et al., 1990). However, the evidence for earlier orogenesis ca.
67 1.78 to 1.75 in the Black Hills (Dahl et al., 1999; Hrncir et al., 2017), as well as high-grade
68 tectonism as early as ca. 1.81 Ga in the Big Sky orogen (Condit et al., 2015), may support the
69 interpretation of Hrncir et al. (2017) that ca. 1.72 Ga activity is a minor overprint on ca. 1.75
70 terminal suturing between Wyoming and Superior. Regardless, in both of these interpretations,
71 Wyoming is a later addition to Laurentia with final suturing post-dating ca. 1.82 Ga
72 amalgamation of Archean provinces with the Trans-Hudson orogen further to the northeast.
73 Overall, the collision of these Archean microcontinents between ca. 1.9 and 1.8 Ga lead to rapid
74 amalgamation of the majority of the Laurentia craton.

75 Crustal growth also progressed in the Paleoproterozoic through accretionary orogenesis. This
76 accretion occurred within the Wopmay orogen through ca. 1.88 Ga arc-continent collision that led
77 to the accretion of the Hottah terrane (the Calderian orogeny) and the subsequent emplacement
78 of the Great Bear magmatic zone from ca. 1.88 to 1.84 Ga (Hildebrand et al., 2009). Coeval with

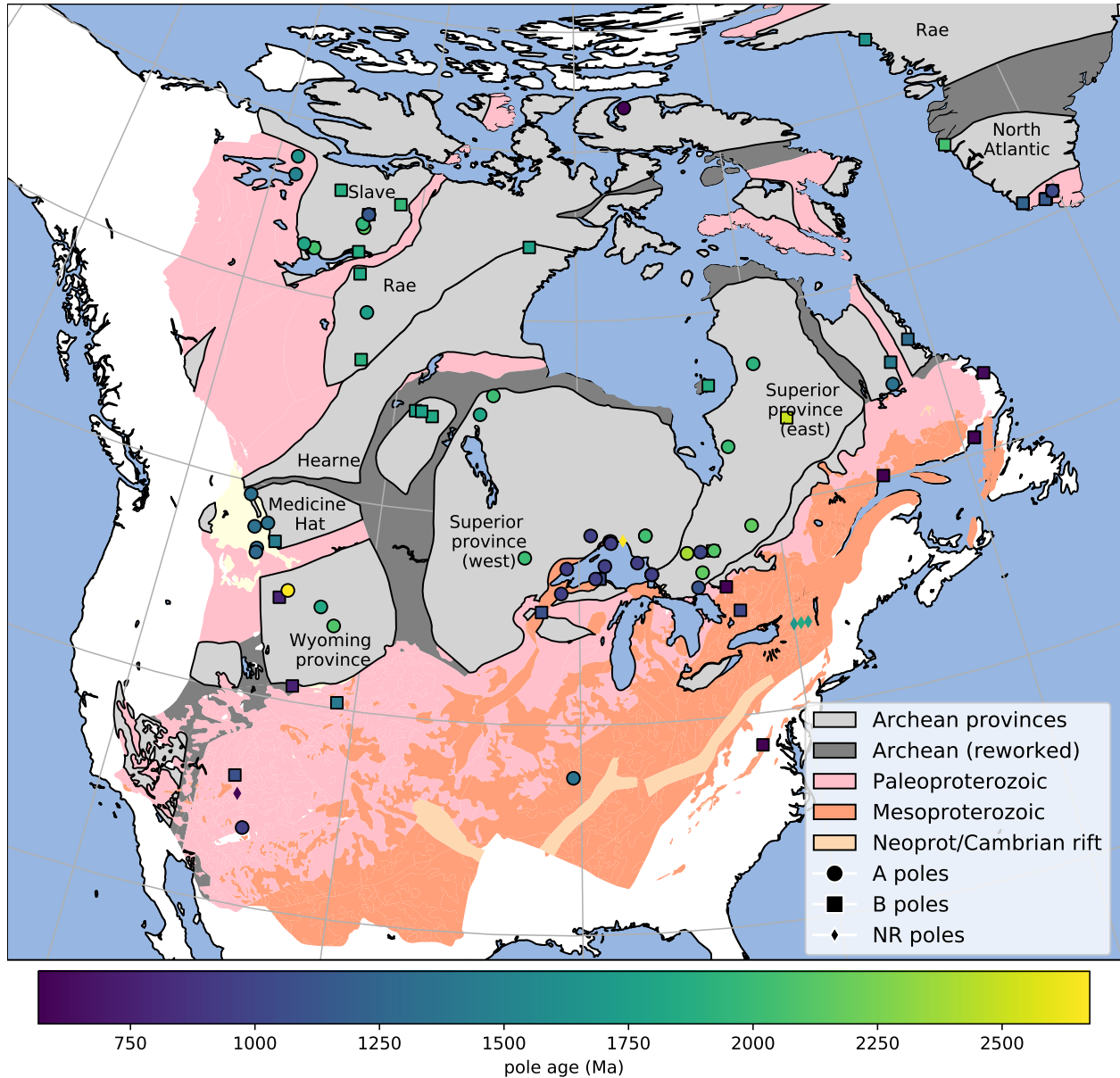


Figure 1. Simplified map of Laurentia showing the location of Archean provinces (labeled with text) and younger Paleoproterozoic and Mesoproterozoic crust (simplified from Whitmeyer and Karlstrom, 2007 with additions for Greenland based on St-Onge et al., 2009). The localities from which the compiled Precambrian paleomagnetic poles were developed are shown and colored by age. The circles (A rated poles) and squares (B rated poles) have been assessed by the Nordic workshop panel.

79 the Trans-Hudson orogeny was the peripheral Penokean orogeny during which both microcontinent
80 blocks (the Marshfield terrane) and arc terranes accreted on the southeastern margin of the west
81 Superior province ca. 1.86 to 1.82 (Schulz and Cannon, 2007). Firm evidence of the end of the
82 orogeny comes from the ca. 1.78 undeformed plutons of the post-Penokean East Central
83 Minnesota Batholith (Holm et al., 2005).

84 In the paleogeographic model framework of Pehrsson et al. (2015), the collisions of provinces
85 and terranes leading up to the Trans-Hudson orogeny mark the initial phase of assembly of the
86 supercontinent Nuna. The Trans-Hudson orogeny itself is taken to be the terminal collision
87 associated with the closure of the Manikewan Ocean that had previously been a large oceanic
88 tract separating the Superior province from the composite Slave+Rae+Hearne+North Atlantic
89 provinces (often referred to as the Churchill domain or plate; e.g. Skipton et al., 2016; Weller and
90 St-Onge, 2017). The Pehrsson et al. (2015) model posits that this period terminal collision not
91 only resulted in the amalgamation of Laurentia, but is also associated with the assembly of the
92 supercontinent Nuna that is hypothesized to include other major Paleoproterozoic cratons
93 including Siberia, Congo/São Francisco, West Africa, and Amazonia (Whitmeyer and Karlstrom,
94 2007; Pehrsson et al., 2015).

95 Following the Trans-Hudson orogeny, the locus of orogenesis migrated to the exterior of
96 Laurentia. This change marks a shift in the predominant style of Laurentia's growth as subsequent
97 crustal growth occurred dominantly through accretion of juvenile crust along the southern and
98 eastern margin of the nucleus of Archean provinces (Whitmeyer and Karlstrom, 2007; Figs. 1 and
99 2). Determining the extent of these belts is complicated by poor exposure of them in the
100 midcontinent relative to the exposure of the Archean provinces throughout the Canadian shield.
101 Major growth of Laurentia following the amalgamation of these Archean provinces occurred
102 associated with the arc-continent collision of the ca. 1.71 to 1.68 Ga Yavapai orogeny. Yavapai
103 orogenesis is interpreted to have resulted from the accretion of a series of arc terranes that
104 collided with each other and Laurentia (Karlstrom et al., 2001). Yavapai accretion was followed
105 by widespread emplacement of granitoid intrusions (Whitmeyer and Karlstrom, 2007). These
106 intrusions are hypothesized to have stabilized the juvenile accreted terranes that subsequently
107 remained part of Laurentia (Whitmeyer and Karlstrom, 2007). Subsequent accretionary

108 orogenesis of the ca. 1.65 to 1.60 Ga Mazatzal orogeny and associated plutonism lead to further
109 crustal growth in the latest Paleoproterozoic (Karlstrom and Bowring, 1988). Laurentia's growth
110 continued in the Mesoproterozoic along the southeast margin through further juvenile terrane and
111 arc accretion. An interval of major plutonism occurred ca. 1.48 to 1.35 Ga leading to the
112 formation of A-type granitoids throughout both Mesoproterozoic and Paleoproterozoic provinces
113 extending from the southwest United States up to the Central Gneiss Belt of Ontario to the
114 northeast of Georgian Bay (Slagstad et al., 2009). This plutonism is likely due to crustal melting
115 within a back-arc region of ca. 1.50 to 1.43 Ga accretionary orogenesis (Bickford et al., 2015).
116 Younger magmatic activity ca. 1.37 Ga of the Southern Granite- Rhyolite Province suggests a
117 similar tectonic setting of accretionary orogenesis at that time (Bickford et al., 2015). While an
118 active margin interpretation with magmatism in back- arc setting has gained traction within the
119 literature with additional data, the tectonic setting is often described as enigmatic given earlier
120 interpretations of an anorogenic setting (see references in Slagstad et al., 2009).

121 Accretionary orogenesis continued along the (south)east margin of Laurentia with the
122 arc-continent collision of the ca. 1.25 to 1.22 Ga Elzevirian orogeny (McLelland et al., 2013). The
123 subsequent ca. 1.19 to 1.16 Ga Shawinigan orogeny is interpreted to be due to the accretion of a
124 terrane comprised of amalgamated arc volcanics and associated metasediments and is followed by
125 a period of tectonic quiescence on the eastern margin of Laurentia until the collision orogenesis of
126 the Grenvillian orogeny (McLelland et al., 2010). In the latest Mesoproterozoic (ca. 1.11 to 1.08
127 Ga), a major intracontinental rift co-located with a large igneous province formed in Laurentia's
128 interior leading to extension within the Archean Superior province and Paleoproterozoic provinces
129 (Cannon, 1992). This Midcontinent Rift led to the formation of a thick succession of volcanics
130 and mafic intrusions that are well-preserved in Laurentia's interior. Midcontinent Rift
131 development ceased as major collisional orogenesis of the Grenvillian orogeny began
132 (Swanson-Hysell et al., 2019). The Grenvillian orogeny was a protracted interval of
133 continent-continent collision (ca. 1.09 to 0.98 Ga) leading to amphibolite to granulite facies
134 metamorphism through the orogen (McLelland et al., 2010). The orogeny is interpreted to have
135 resulted in the development of a thick orogenic plateau (Rivers, 2008).

136 There is significantly less preserved crustal growth on the western margin of Laurentia (Fig. 1)

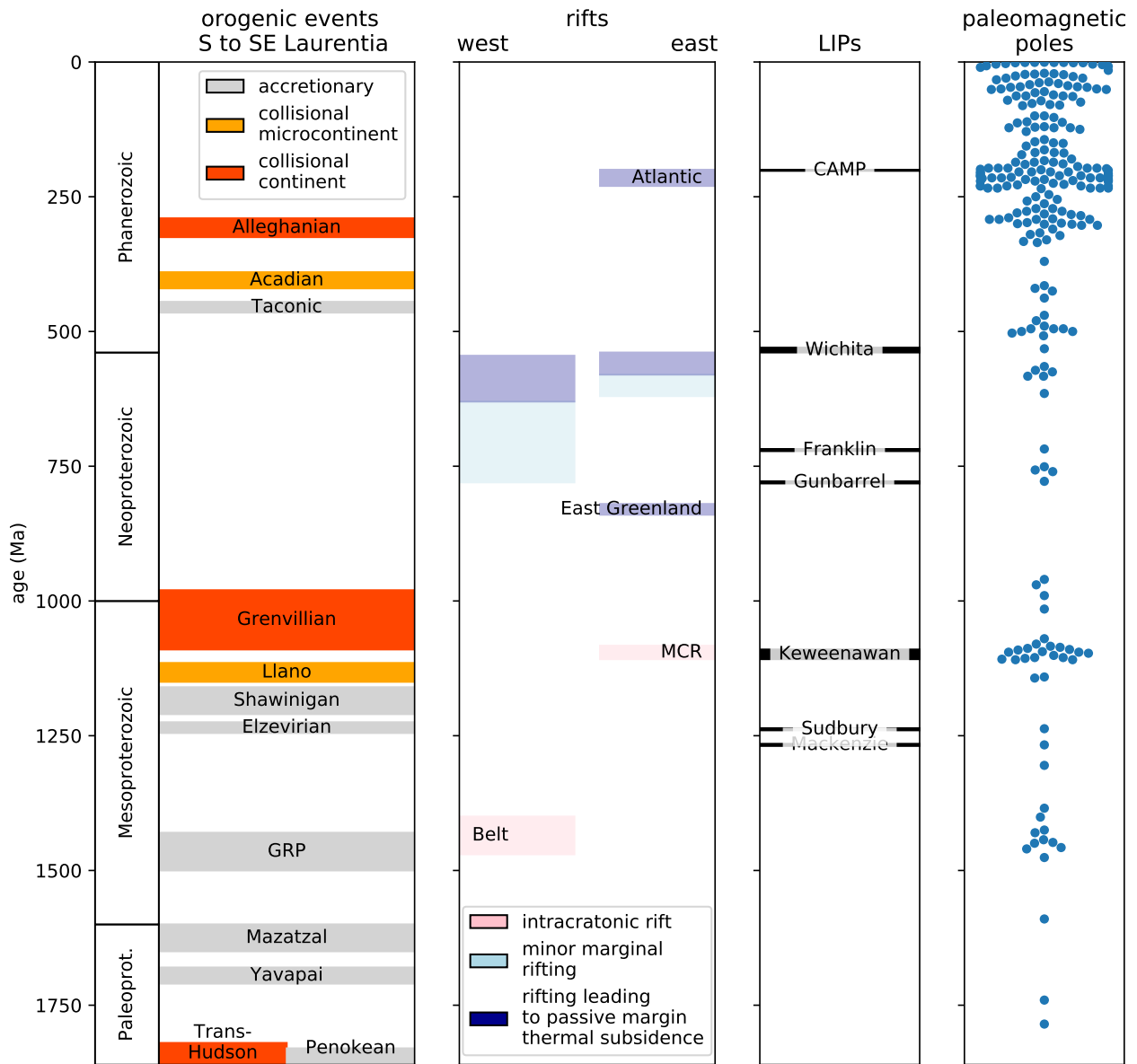


Figure 2. Simplified timeline of Laurentia's tectonic history over the past ~1.8 billion years. Brief summaries and references related to the orogenic and rifting episodes are given in the text. A timeline of large igneous provinces (LIPs) associated with typically brief and voluminous (or interpreted to be voluminous) volcanism is also shown. The interpreted age of paleomagnetic poles for Laurentia (not including separated terranes) compiled in this study for the Proterozoic and in Torsvik et al. (2012) for the Phanerozoic is shown.

137 and the Mesoproterozoic tectonic history is not as well elucidated as on the southern to eastern
138 margin. The 15 to 20 km thick package of sedimentary rocks of the Belt-Purcell Supergroup is
139 associated with a ca. 1.47 to 1.40 intracontinental rift – the tectonic setting of which is debated.
140 Hoffman (1989) proposed that it may be a remnant back-arc basin trapped within a continent,
141 while others envision it as being associated with continental rifting along the margin associated
142 with separation of a conjugate continent (Jones et al., 2015). This region is interpreted to have
143 been subsequently deformed during a ca. 1.36 to 1.33 event known as the East Kootenay orogeny
144 (McMechan and Price, 1982; Nesheim et al., 2012; McFarlane, 2015).

145 This late Paleoproterozoic and Mesoproterozoic tectonic history provides significant constraints
146 on paleogeographic reconstructions. In particular, the long-lived history of accretionary orogenesis
147 along the southeast (present-day coordinates) of Laurentia from the initiation of the Yavapai
148 orogeny (ca. 1.71 Ga) to the end of the Shawinigan orogeny (ca. 1.06 Ga) requires a long-lived
149 open margin without a major conjugate continent until the time of terminal Grenvillian orogeny
150 collision (Karlstrom et al., 2001). This constraint is incorporated into models such as that of
151 Zhang et al. (2012) and Pehrsson et al. (2015) which maintain a long-lived convergent margin
152 throughout the Mesoproterozoic, but in some reconstructions other continental blocks are
153 reconstructed into positions that are seemingly incompatible with this record of accretionary
154 orogenesis (e.g. Amazonia in Elming et al., 2009). The high-grade metamorphism associated with
155 the Ottawan phase of the Grenvillian orogeny itself requires a collision between Laurentia and
156 (an)other continent(s) ca. 1080 Ma – the geological observation of which first lead to the
157 formulation of the hypothesis of the supercontinent Rodinia (Hoffman, 1991). Evidence of
158 large-scale continent-continent collision at the time of the Ottawan Phase of the Grenvillian
159 orogeny is recorded in Texas, up through the Blue Ridge Appalachian inliers, through Ontario
160 and up to the Labrador Sea. This extensive and major collision orogenic history recorded in
161 Laurentia remains a strong piece of evidence that a supercontinent or (proto)supercontinent
162 formed at the 1.0 Ga Mesoproterozoic to Neoproterozoic transition. The term Grenville orogeny
163 or Grenville belt is used rather loosely throughout much of the literature to refer to any late
164 Mesoproterozoic orogenic belt. The timeline of orogenesis on the Laurentia margin has more
165 nuanced constraints than this usage and these constraints can be comparatively assessed when

¹⁶⁶ evaluating potential conjugate continents to Laurentia associated with the orogen (Fig. 2).

¹⁶⁷ The subsequent Neoproterozoic tectonic history of Laurentia is dominantly a record of rifting
¹⁶⁸ (Fig. 2). Along the western margin of Laurentia, small-scale rifting occurred ca. 780 to 720 Ma
¹⁶⁹ leading to deposition in basins that is recorded from the Death Valley region of SW Laurentia up
¹⁷⁰ to the Mackenzie Mountains of NW Laurentia (Macdonald et al., 2012; Rooney et al., 2017).
¹⁷¹ However, this extensional basin development is relatively minor and predates the more significant
¹⁷² rifting that lead to passive margin thermal subsidence that did not occur until the Ediacaran
¹⁷³ Period (closer to the ca. 539 Ma Neoproterozoic-Phanerozoic boundary; Bond et al., 1984; Levy
¹⁷⁴ and Christie-Blick, 1991). The emplacement of the ca. 780 Ma Gunbarrel large igneous province
¹⁷⁵ along this margin and the subsequent extension recorded in the basins is commonly interpreted to
¹⁷⁶ be associated with the break-up of Laurentia and a conjugate continent to the western margin. If
¹⁷⁷ this interpretation is correct, it is unclear why there would be minimal thermal subsidence until
¹⁷⁸ the Ediacaran (post 635 Ma as in Levy and Christie-Blick, 1991 and Witkosky and Wernicke,
¹⁷⁹ 2018). The geological evidence therefore supports active tectonism along the western margin of
¹⁸⁰ Laurentia, but suggests that more dramatic lithospheric thinning occurred later than the timing
¹⁸¹ of rifting typically implemented in models of Rodinia break-up. One possibility, along the lines of
¹⁸² that proposed in Ross (1991), is that ca. 780 Ma extensional tectonism is an inboard record of
¹⁸³ rifting and passive margin development that occurred further outboard. In this model,
¹⁸⁴ subsequent continent rifting that drove lithospheric thinning, perhaps associated with the
¹⁸⁵ departure of a microcontinent fragment rather than an already departed major conjugate
¹⁸⁶ continent, would be the cause of Ediacaran to Cambrian thermal subsidence. The margin that
¹⁸⁷ did experience large-scale rifting and associated passive margin thermal subsidence earlier in the
¹⁸⁸ Neoproterozoic is the northeast Greenland margin (Fig. 2). Available geochronological constraints
¹⁸⁹ and thermal subsidence modeling indicate ca. 820 Ma rifting followed by thermal subsidence of a
¹⁹⁰ stable platform (Maloof et al., 2006; Halverson et al., 2018). These data suggest that conjugate
¹⁹¹ continental lithosphere rifted away from northeast Greenland ca. 820 Ma.

¹⁹² Extensive rifting that was followed by thermal subsidence occurred along the southeast to east
¹⁹³ Laurentia margin leading up to the Neoproterozoic-Phanerozoic boundary and is interpreted to be
¹⁹⁴ associated with the opening of the Iapetus ocean. A record of this rifting is preserved as rift

195 basins that were part of failed arms (Rome trough, Reelfoot rift and Oklahoma aulacogen; Fig. 1)
196 as well as prolonged Cambrian to Ordovician passive margin thermal subsidence along the margin
197 (Bond et al., 1984; Whitmeyer and Karlstrom, 2007). The age of igneous intrusions that have
198 been interpreted to be rift-related play a significant role in interpretations of this history such as
199 in the rift development model of Burton and Southworth (2010). In this model,
200 spatially-restricted rifting occurs ca. 760 to 680 Ma in the region of modern-day North Carolina
201 and Virginia. Rifting ca. 620 to 580 Ma initiates in the region from modern-day New York to
202 Newfoundland and by ca. 580 to 550 Ma rifting extends along the length of Laurentia's eastern
203 margin. The last phases of this rifting appears to be associated with the separation of the
204 Argentine pre-Cordillera Cuyania terrane (Dickerson and Keller, 1998). Cuyania is widely
205 interpreted be a rifted fragment of SE Laurentia that separated associated with this early
206 Cambrian rifting and subsequently became part of Gondwana when it collided with other terranes
207 in the vicinity of the Rio de Plata craton during the Ordovician Famatinian orogeny (Martin
208 et al., 2019). As with other rifts, it is difficult to distinguish the separation of a cratonic fragment
209 as a microcontinent from the rifting of a major craton as the record that lingers on the craton is
210 similar. One interpretation is that there was successful break-up along the eastern margin during
211 the ca. 580 to 550 Ma interval of rifting prior to the ca. 539 Oklahoma aulacogen rifting that
212 liberated the Cuyania microcontinent. The Maz- Arequipa-Rio Apa (MARA) block with which
213 Cuyania collided (Martin et al., 2019) is likely a product of such rifting. Orogenesis between the
214 MARA block and the Rio de Plata and Kalahari in the ca. 530 Ma Pampean orogeny (Casquet
215 et al., 2018) predated the collision of Cuyania during the ca. 460 Ma Famatinian orogeny in West
216 Gondwana (Rapalini, 2018).

217 The eastern margin of Laurentia then went through the cycle of Appalachian orogenesis. As is
218 visualized in Figure 2, there are parallels between the Grenville orogenic interval and the
219 Appalachian orogenic interval in that there was a period of arc-continent collision (Shawinigan
220 orogeny in the Grenville interval; Taconic orogeny in the Appalachian interval) followed by
221 microcontinent accretion (Llano in the Grenville interval; Acadian in the Appalachian interval)
222 that culminated in large-scale continent-continent collision (Grenvillian orogeny in the Grenville
223 interval; Alleghanian in the Appalachian interval). These similarities are the consequence of an

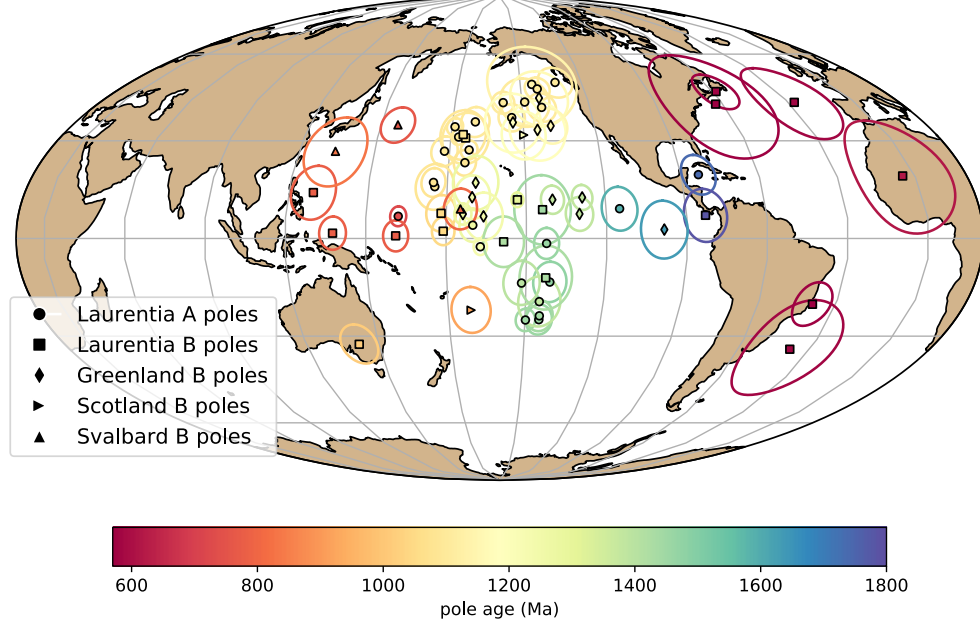
²²⁴ active margin facing an ocean basin that was progressively consumed until its consumption
²²⁵ resulted in continent-continent collision. In the case of the Grenville interval, this terminal
²²⁶ collision is interpreted to be associated with the assembly of the supercontinent Rodinia and in
²²⁷ the Appalachian interval it is interpreted to be associated with the assembly of the supercontinent
²²⁸ Pangea.

²²⁹ Even without considering other continents on Earth, the geological record of Paleoproterozoic
²³⁰ collisional of Archean provinces combined with accretionary orogenesis at that time and through
²³¹ the rest of the Paleoproterozoic and Mesoproterozoic Eras provides strong evidence for mobile
²³² plate tectonics driving Laurentia's evolution throughout the past 2 billion years. This tectonic
²³³ history inferred from geological data can be enhanced through integration with the paleomagnetic
²³⁴ record.

²³⁵ 3.3 Paleomagnetic pole compilation

²³⁶ In this chapter, I focus on the compilation of paleomagnetic poles developed through the Nordic
²³⁷ Paleomagnetism Workshops with some additions and modifications (Fig. 3 and Table 2). The
²³⁸ Nordic Paleomagnetism Workshops have taken the approach of using expert panels to assess
²³⁹ paleomagnetic poles and assign them grades meant to convey the confidence that the community
²⁴⁰ has in these results (Evans et al., this volume). While many factors associated with
²⁴¹ paleomagnetic poles can be assessed quantitatively through Fisher statistics and the precision of
²⁴² geochronological constraints, other aspects such as the degree to which available field tests
²⁴³ constrain the magnetization to be primary require expert assessment. The categorizations used by
²⁴⁴ the expert panel are 'A' and 'B' with the last panel meeting occurring in Fall 2017 in Leirubakki,
²⁴⁵ Iceland. An 'A' rating refers to poles that are judged to be of such high-quality that they provide
²⁴⁶ essential constraints that should be satisfied in paleogeographic reconstructions. A 'B' rating is
²⁴⁷ associated with poles that are judged to likely provide a high-quality constraint, but have some
²⁴⁸ deficiency such as remaining ambiguity in the demonstration of primary remanence or the
²⁴⁹ quality/precision of available geochronologic constraints. Additional poles that were not given an
²⁵⁰ 'A' or 'B' classification at the Nordic Workshops are referred to as not-rated ('NR'). These
²⁵¹ additional poles are taken from the Paleomagia database (Veikkolainen et al., 2014). Many of

Poles for Laurentia (post-Paleoproterozoic amalgamation; with terranes)



Poles for Laurentia (pre-Paleoproterozoic amalgamation)

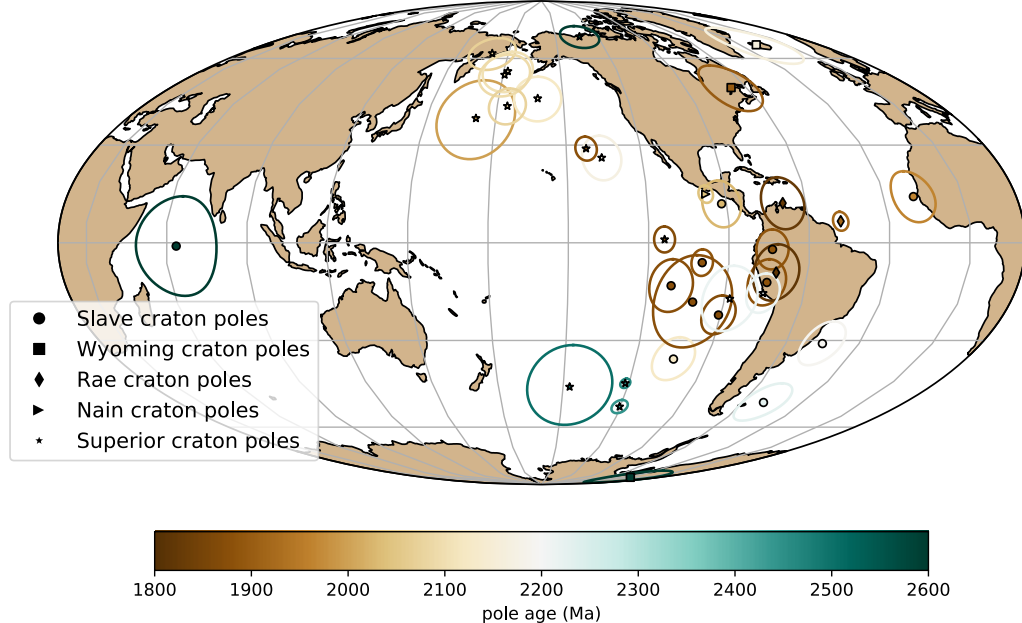


Figure 3. Top panel: Paleomagnetic poles from 1800 to 560 Ma for Laurentia (including Greenland, Scotland and Svalbard). Bottom panel: Paleomagnetic data for Archean Provinces prior to the amalgamation of Laurentia.

252 these poles in the Paleomagia database are quite valuable for reconstruction and should not be
253 dismissed from being considered in paleogeographic reconstructions. However, there are
254 ambiguities associated with many of such poles not given Nordic ‘A’ or ‘B’ ratings in terms of
255 how well the nature of the remanence is constrained including its age. For example, there are rich
256 data associated with intrusive and metamorphic lithologies of the Grenville Province that are the
257 available paleomagnetic constraints for Laurentia at the Mesoproterozoic-Neoproterozoic
258 boundary. However, the ages of the remanence associated with these poles is complicated by the
259 reality that the magnetization was acquired during exhumation and such cooling ages are more
260 difficult to robustly constrain than the ages of remanence associated with dated eruptive units or
261 shallow-level intrusions. As a result, the vast majority of Grenville Province poles are not given
262 an ‘A’ or ‘B’ rating with the exception of the ‘B’ rated pole from the ca. 1015 Ma Haliburton
263 intrusions. However, while any one of these Grenville poles could be interpreted to suffer from
264 large temporal uncertainty, the overall preponderance of poles in a similar location at the time
265 suggests that they need to be taken seriously within any paleogeographic reconstruction of
266 Laurentia (although note an alternative view of an allochthonous origin put forward by Halls
267 et al. (2015) is discussed below). In this compilation, the poles of Brown and McEnroe (2012)
268 from the Adirondack highlands are used wherein the magnetic mineralogy and associated relative
269 ages of remanence are well-constrained (Table 2). Additional not-rated poles included in the
270 present compilation is the new pole for the ca. 1144 Ma Ontario lamprophyre dykes (Piispa et al.,
271 2018) that strengthens the position of Laurentia at the time and coincides with the position of the
272 poles from the ca. 1140 Ma Abitibi dikes (Ernst and Buchan, 1993). This pole will likely receive
273 an ‘A’ rating when assessed at the next Nordic paleomagnetism workshop. Poles from the
274 Neoproterozoic Chuar Group as presented in Eyster et al. (2019) are also included.

275 3.4 Differential motion before Laurentia amalgamation

276 Prior to the termination of the Trans-Hudson orogeny (before 1.8 Ga), paleomagnetic poles need
277 to be considered with respect to the individual Archean provinces. For the Superior province, an
278 additional complexity is that paleomagnetic poles from Siderian to Rhyacian Period (2.50 to 2.05
279 Ga) dike swarms, as well as deflection of dike trends, support an interpretation that there was

280 substantial Paleoproterozoic rotation of the western Superior province relative to the eastern
281 Superior province across the Kapuskasing Structural Zone (Bates and Halls, 1991; Evans and
282 Halls, 2010). This interpretation is consistent with the hypothesis of Hoffman (1988) that the
283 Kapuskasing Structural Zone represents major intracratonic uplift related to the Trans-Hudson
284 orogeny. Evans and Halls (2010) propose an Euler rotation of (51°N, 85°W, -14°CCW) to
285 reconstruct western Superior relative to eastern Superior and interpret that the rotation occurred
286 in the time interval of 2.07 to 1.87 Ga. I follow this interpretation and group the poles into
287 Superior (West) and Superior (East). Uncertainty remains with respect to whether the ca. 1.88
288 Ga Molson dikes pole pre-dates or post-dates this rotation (Evans and Halls, 2010) and thus for
289 the time being should be considered solely in the western Superior province reference frame.

290 There are poles in the compilation for the Slave, Wyoming, Rae, Superior and North Atlantic
291 provinces prior to Laurentia amalgamation (Fig. 3 and Table 2). Overall, these data provide an
292 opportunity to re-evaluate the paleomagnetic evidence for relative motions between Archean
293 provinces prior to Laurentia assembly. A lingering question raised in Hoffman (1988) that still
294 remains is to what extent the Archean provinces each had independent drift histories with
295 significant separation or shared histories before experiencing fragmentation and reamalgamation.
296 The strongest analysis in this regard comes from comparisons between paleomagnetic poles
297 between the Superior and Slave provinces (Buchan et al., 2009; Mitchell et al., 2014; Buchan
298 et al., 2016). High-quality paleomagnetic poles from these two provinces provide strong support
299 for differential motion between the Superior and Slave provinces between 2.2 and 1.8 Ga with the
300 two provinces not being in their modern-day relative orientation to one another and having
301 distinct pole paths as constrained by 5 time periods of nearly coeval poles from 2.23 and 1.89 Ga
302 (Fig. 4; Buchan et al., 2016. These data provide paleomagnetic support for the Superior and
303 Slave provinces having independent histories of differential motion. The data also support the
304 hypothesis that the Trans-Hudson orogeny is the result of terminal collision associated with the
305 closure of an ocean basin between the Superior province and the Hearne+Rae+Slave provinces.
306 Reconstructions developed for this chapter of the Superior and Slave provinces using these poles
307 are shown in Figure 4 and illustrate the difference in implied orientation and paleolatitude that
308 results from these well-constrained poles.

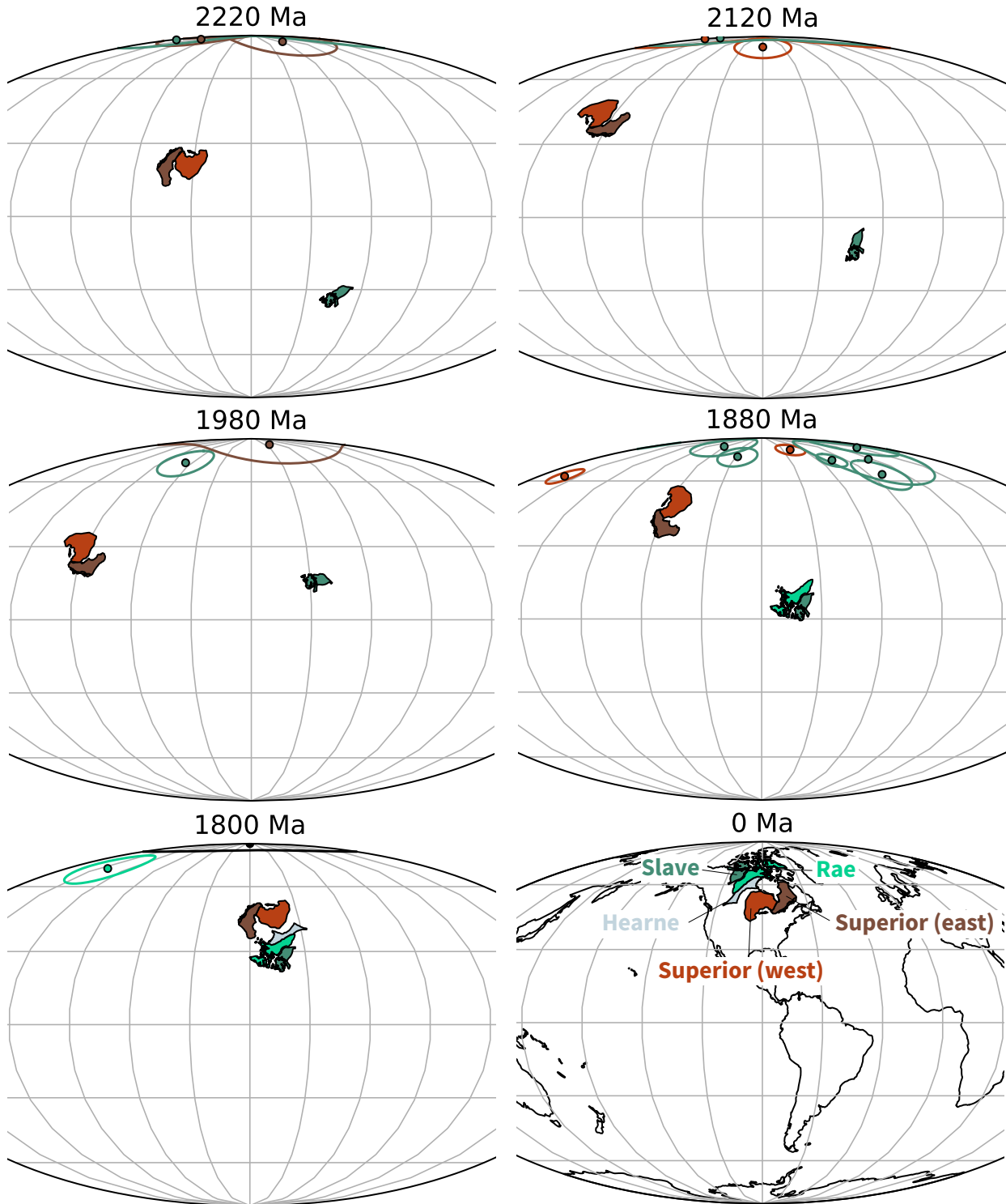


Figure 4. Paleogeographic reconstructions developed using poles from the Superior, Slave and Rae provinces. The polarity options that are chosen for the provinces are those that minimize total apparent polar wander path length. Paleomagnetic poles are shown colored to match their respective province with these provinces shown in present-day coordinates and labeled in the 0 Ma panel. Poles with ages that are within 25 million years of the given time slice are shown. The relatively well-resolved pole paths from the Superior and Slave provinces (Fig. 3) that are utilized for these reconstructions provide strong support for differential plate tectonic motion between 2220 and 1850 Ma.

³⁰⁹ **3.5 Paleogeography of an assembled Laurentia**

³¹⁰ Following the amalgamation of the Archean provinces in Laurentia ca. 1.8 Ga, poles from each
³¹¹ part of Laurentia can be considered to reflect the position of the entire composite craton. It is
³¹² worth considering the possibility that poles from zones of Paleoproterozoic and Mesoproterozoic
³¹³ accretion could be allochthonous to the craton. Halls (2015) argued that this was the case for late
³¹⁴ Mesoproterozoic and early Neoproterozoic poles from east of the Grenvillian allochthon boundary
³¹⁵ fault. However, the majority of researchers have considered these poles to post-date major
³¹⁶ differential motion and be associated with cooling during collapse of a thick orogenic plateau
³¹⁷ developed during continent-continent collision (e.g. Brown and McEnroe, 2012). Poles with a
³¹⁸ B-rating are also included in the composite that come from Greenland, Svalbard and Scotland.
³¹⁹ These terranes were once part of contiguous Laurentia, but have subsequently rifted away. These
³²⁰ poles need to be rotated into the Laurentia reference frame prior to use for tectonic
³²¹ reconstruction and I apply the rotations shown in Table 1. The Euler pole and rotation is quite
³²² well-constrained for Greenland as it is associated with recent opening of Baffin Bay and the
³²³ Labrador Sea (for which the rotation of Roest and Srivastava, 1989 is used). The reconstruction
³²⁴ of Scotland is associated with the opening of the Atlantic (for which the rotation employed by
³²⁵ Torsvik and Cocks, 2017 is used) which is well-constrained but has more uncertainty associated
³²⁶ with the Euler pole than that for Greenland. The reconstruction of Svalbard is more challenging
³²⁷ given a multi-state tectonic history involving both translation within the Caledonides and
³²⁸ subsequent rifting. The preferred Euler of Maloof et al. (2006) is used here. This Euler is
³²⁹ designed, in particular, to honor the high degree of similarity between Tonian sediments in East
³³⁰ Greenland (Hoffman et al., 2012) and those of East Svalbard (Maloof et al., 2006) and to
³³¹ reconstruct East Svalbard to be aligned with these correlative sedimentary rocks.

³³² Through the Proterozoic, there are intervals where there are abundant paleomagnetic poles
³³³ that constrain Laurentia's position and intervals when the record is sparse (shown colored by age
³³⁴ in Fig. 3). To further visualize the temporal coverage of the poles and to summarize the motion,
³³⁵ implied paleolatitudes for an interior point on Laurentia are shown in Figure 5. The ages of the
³³⁶ utilized paleomagnetic poles are also shown in comparison to the simplified summary of tectonic
³³⁷ events in Figure 2. Both collisional and extensional tectonism can result in the formation of

338 lithologies that can be used to develop paleomagnetic poles either as a result of basin formation,
339 magmatism or both. In addition, intraplate magmatism resulting from plume-related
340 large-igneous provinces can lead to paleomagnetic poles in periods that are otherwise
341 characterized by tectonic quiescence (e.g. the ca. 1267 Ma Mackenzie LIP; Fig. 2).

342 Intracontinental rifts have led to the highest density of poles both in the case of the ca. 1.4 Ga
343 Belt Supergroup and the ca. 1.1 Ga Midcontinent Rift (Fig. 2). The quality and resolution of the
344 record from the Midcontinent Rift is aided by the voluminous magmatism that occurred in
345 conjunction with basin formation that enables the development of well-calibrated apparent polar
346 wander path (Swanson-Hysell et al., 2019). The late Tonian Period also has a number of poles
347 including the Gunbarrel LIP (ca. 780 Ma) and Franklin LIP (ca. 720 Ma), as well as
348 similarly-aged sedimentary rocks from western Laurentia basins (Eyster et al., 2019). Overall,
349 there is internal consistency among the paleomagnetic poles within intervals for which there is
350 high-resolution coverage. These data result in progressive paths such as ascending up to the
351 Logan Loop, down the Keweenawan Track (Swanson-Hysell et al., 2019) to the Grenville Loop
352 prior to a temporal gap before the late Tonian (ca. 775 to 720 Ma) path (Eyster et al., 2019).

353 Data from other terranes add resolution to the record. In particular, data from Greenland
354 adds 12 poles between 1385 and 1160 Ma when there are only 4 poles from mainland Laurentia.
355 Given that the rotation between Greenland and mainland Laurentia is well-constrained (Table 1),
356 once rotated these poles can be used for reconstruction of the entire continent. The reliability of
357 this approach gains credence through the good agreement between the ca. 1633 Ma Melville Bugt
358 diabase dykes pole from Greenland (Halls et al., 2011) and the ca. 1590 Ma Western Channel
359 diabase pole of mainland Laurentia (Irving and Park, 1972). Similarly, there is good agreement
360 between the ca. 1267 Ma Mackenzie dykes pole of Laurentia (Buchan et al., 2000) and coeval
361 poles from Greenland such as the ca. 1275 Ma North Qoroq intrusives (Piper, 1992) and Kungnat
362 Ring dyke (Piper, 1977). Furthermore, the Greenland poles with ages that fall between the ca.
363 1237 Ma Sudbury dikes and ca. 1143 Ma lamprophyre dykes pole of mainland Laurentia are
364 consistent with constraints on either side from the mainland while filling in the ascending limb of
365 the path leading up to the apex of 1140 to 1108 Ma poles known as the Logan Loop.

366 An exception to this overall agreement between poles from Greenland and mainland Laurentia

367 occurs ca. 1382 Ma. There are poles of this age from Greenland associated with the Zig-Zag Dal
368 basalts and related intrusions (Marcussen and Abrahamsen, 1983; Abrahamsen and Van Der Voo,
369 1987). However, these poles are in a distinct location from poles of similar age associated with the
370 Belt Supergroup (e.g. the McNamara Formation and Pilcher/Garnet Range and Libby
371 Formations; Elston et al., 2002). Additionally, the older Belt Supergroup poles form a more
372 southerly population than time-equivalent poles from elsewhere in Laurentia such as the Mistastin
373 Pluton. There are potential complications associated with the Belt Supergroup being exposed
374 within thrust sheets with significant Cenozoic Mesozoic and Cenozoic deformation. However,
375 vertical axis rotations of the Belt region are not able to bring the Belt poles into agreement with
376 those from Laurentia or Greenland nor is translation away from the craton. Another potential
377 complication is that the remanence used for the development of the Belt Supergroup resides in
378 hematite. As a result, there is the potential for inclination-flattening within the sedimentary rocks
379 from which poles are developed. However, applying a moderate inclination factor of $f = 0.6$ also
380 does not bring the poles into congruence with the Zig-Zag basalts. There is the potential that the
381 hematite could be the result of post-depositional oxidation (the remanence of the Purcell lavas
382 pole is also held by hematite) however the overall coherency of the pole directions and the
383 presence of reversals has been taken as evidence that the remanence is primary (Elston et al.,
384 2002). At present, it is unclear which poles are a better representation of Laurentia's position ca.
385 1400 Ma.

386 Another challenging portion of the Laurentia record is that for the Ediacaran Period where
387 there is little consistency between poles of similar age (Figs. 3 and 5). As a result, there are poles
388 that imply both low-latitude and high-latitude positions of Laurentia between 615 and 565 Ma.
389 One explanation for these variable pole positions is that they are the result of large-scale
390 oscillatory true polar wander in the Ediacaran that has influenced poles in Baltica and West
391 Africa as well (McCausland et al., 2007; Robert et al., 2017). Another possibility is that the lack
392 of congruency between poles in this point in the record is due to a particularly weak and
393 non-dipolar geomagnetic field (Abrajevitch and Van der Voo, 2010; Bono et al., 2019). Regardless
394 of mechanism, the Ediacaran data stand out as anomalous relative to the coherency of the rest of
395 the poles in the composite (Fig. 5).

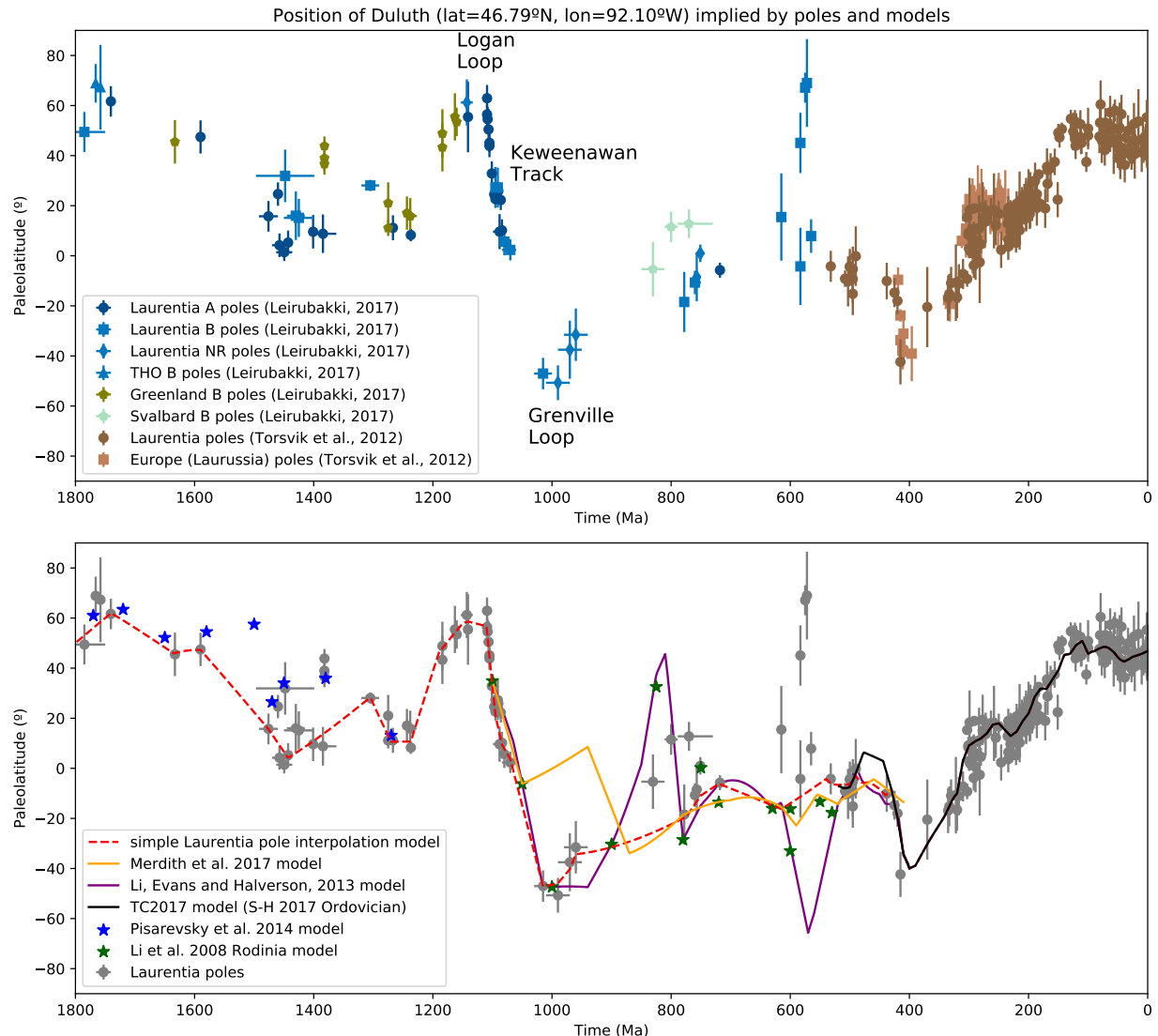


Figure 5. Top panel: Paleolatitude implied by paleomagnetic poles from Laurentia and associated blocks for Duluth (lat=46.79°N, lon=92.10°W). The paleomagnetic poles are compiled in Table 2. Bottom panel: Paleolatitude implied by Laurentia poles compared with that implied by published paleogeographic models and the simple Laurentia model used in this chapter for the reconstructions in Figure 6.

396 Synthesizing the compilation of paleomagnetic poles for Laurentia into a composite path over
397 the past 1.8 billion years presents a challenge given the highly variable temporal coverage. The
398 method typically applied in the Phanerozoic is to develop synthesized pole paths either through
399 fitting spherical splines through the data or calculating binned running means where the Fisher
400 mean of poles within a given interval are calculated (Torsvik et al., 2012). Applying such an
401 approach can reduce the effect of spurious poles in regions of high data density where seeking to
402 satisfy every mean pole position would result in jerky motion.

403 A synthesized pole path for Laurentia is developed here and used to develop a continuous
404 paleogeographic reconstruction of Laurentia constrained by the compilation of paleomagnetic
405 poles. The paleolatitude implied by this continuous model is shown in Figure 5. This path is
406 based on Laurentia data alone which means that it is poorly constrained through intervals of
407 sparse data (950-850 Ma for example). One could use interpretations of paleogeographic
408 connections with other cratons (e.g. Baltica in the early Neoproterozoic) to fill in such portions of
409 the path, however the result then becomes model-dependent without being constrained by data
410 from Laurentia itself. In portions of the record with a more dense record of poles, such as ca.
411 1450, a calculated running mean is used to integrate constraints from multiple poles. This
412 method follows the approach taken in the Phanerozoic (e.g. Torsvik et al., 2012 wherein all poles
413 within a 20 Myr interval are averaged with the interval than progressively moved forward in 10
414 Myr steps. When there are isolated ‘A’ grade poles without other temporally-similar poles, these
415 poles are fully satisfied in model. Where there are no constraints a simple interpolation between
416 constraints is made. While data from Scotland and Svalbard are associated with Laurentia, the
417 Scotland poles are poorly constrained in time and the Svalbard rotation to Laurentia is uncertain.
418 These poles are not utilized in the simple Laurentia model which means that the model as shown
419 does not include oscillatory true polar wander interpreted to have occurred ca. 810 and 790 Ma
420 based on data from Svalbard (Maloof et al., 2006). The model of Li et al. (2013) shown in Figure
421 5 does seek to incorporate this true polar wander while also incorporating an interpretation of the
422 paleomagnetic pole record from South China.

423 One downside of a running mean approach is that it pulls the mean to regions of high data
424 density. As was shown in Swanson-Hysell et al. (2019), this behavior can reduce motion along an

425 apparent polar wander path. As a result, for the portion of the reconstruction during the interval
426 of time ca. 1110 to 1070 Ma where there is high data density from the Midcontinent Rift, I utilize
427 an Euler pole inversion from Swanson-Hysell et al. (2019).

428 Paleogeographic snapshots for the past position of Laurentia reconstructed using this synthesis
429 of the paleomagnetic poles are shown in Figure 6. These reconstructions use the tectonic elements
430 as defined by Whitmeyer and Karlstrom (2007) with these elements being progressively added
431 associated with Laurentia’s accretionary growth. As a reminder to the reader, paleomagnetic
432 poles provide constraints on the paleolatitude of a continental block as well as its orientation
433 (which way was north relative to the block). While they provide constraints in this regard, they
434 do not provide constraints in and of themselves for the longitudinal position of the block. Other
435 approaches to obtain paleolongitude utilize geophysical hypotheses such as assuming that large
436 low shear velocity provinces have been stable plume-generating zones in the lower mantle to
437 which plumes can be reconstructed (Torsvik et al., 2014) or that significant pole motion in certain
438 time intervals is associated with true polar wander axes that switch through time in conjunction
439 with the supercontinent cycle (Mitchell et al., 2012). In Figure 6, Laurentia is centered on the
440 longitudinal position of Duluth with the orientation and paleolatitude being constrained by the
441 paleomagnetic pole compilation as synthesized in the simple Laurentia pole interpolation model.
442 The continuous paleolatitude implied by this model is shown as the simple Laurentia pole
443 interpolation mode in Figure 5.

444 3.6 Comparing paleogeographic models to the paleomagnetic compilation

445 Developing comprehensive global continuous paleogeographic models is a major challenge given
446 the need to integrate and satisfy diverse geological and paleomagnetic data types. Continually
447 improving constraints related to tectonic setting from improved geologic and geochronologic data
448 need to be carefully integrated with the database of paleomagnetic poles. Paleomagnetic poles
449 compilations themselves are evolving with better data and improved geochronology. Efforts such
450 as this volume are therefore essential to present the state-of-the-art in terms of existing
451 constraints that can be used to evaluate current models and set the stage for future progress in
452 Precambrian paleogeography.

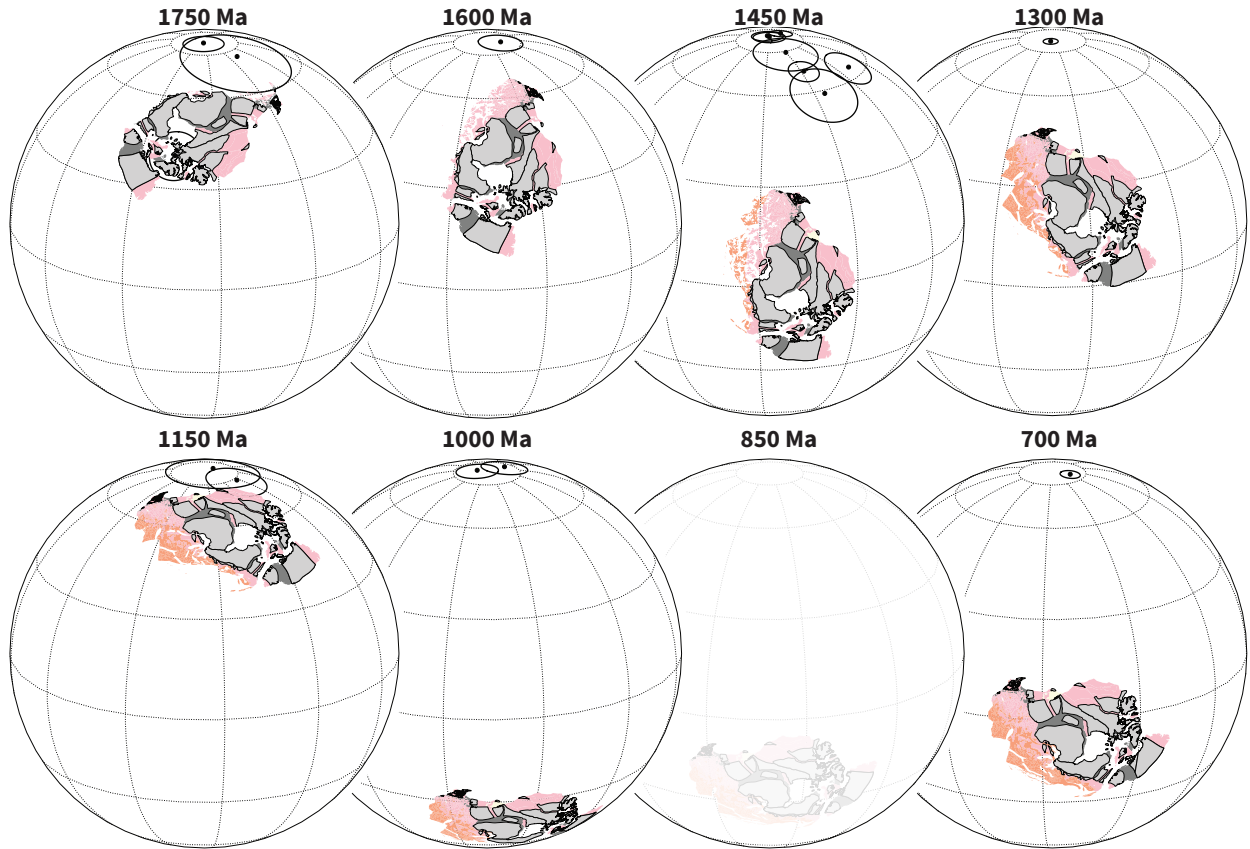


Figure 6. Paleogeographic reconstructions of Laurentia at time intervals through the Proterozoic that are well-constrained by paleomagnetic data. These reconstructions use the simple Laurentia pole interpolation model that is shown in Figure 5 and use this model to reconstruct the tectonic elements of Whitmeyer and Karlstrom (2007) shown in Figure 1. Modern coastlines are maintained in these polygons so that the rotated orientations can be interpreted by the reader in comparison to Figure 1. Paleomagnetic poles within 25 million years of each reconstruction time are plotted. All reconstructions have poles within such a time frame that provide constraints with the exception of the 850 Ma reconstruction which is shown faintly given this relative uncertainty in Laurentia's position.

453 There is an overall lack of models in the literature for the Proterozoic have published
454 continuous rotation parameters that can be compared to the compilation of paleomagnetic poles
455 presented herein. The approach in the community for many years has been to publish models as
456 snapshots at given time intervals presented in figures without publishing continuous rotation
457 parameters although some studies have published the Euler rotations associated with specified
458 times. With the further adoption of software tools such as GPlates, there has been significant
459 progress in the publication of continuous paleogeographic models constrained by paleomagnetic
460 poles through the Phanerozoic (540 Ma to present; e.g. Torsvik et al., 2012).

461 An exception to the paucity of published continuous paleogeographic models for the
462 Precambrian is the Neoproterozoic model of Merdith et al. (2017) which is shown in comparison
463 to the constraints for Laurentia in Figure 5. The extent to which the implied position of
464 Laurentia in Merdith et al. (2017) is consistent with the compiled paleomagnetic constraints can
465 be visualized in Figure 5. As noted above, the development of such models is challenging and the
466 researchers need to balance varying constraints. The focus here will be on the extent to which
467 this model satisfies the available paleomagnetic poles for Laurentia. The model does not honor
468 the Grenville loop (e.g. go to moderately high southerly latitudes ca. 1000 Ma) which is a
469 striking departure from the paleomagnetic record and standard paleogeographic models.
470 Additionally, the implemented plate motion strays from the younger poles of the Keweenawan
471 Track and does not honor the Franklin LIP pole Denyszyn et al. (2009b) despite its ‘A’ Nordic
472 rating. The Franklin pole is taken to be a key constraint at the Tonian/Cryogenian boundary
473 that provides evidence of the supercontinent Rodinia being equatorial and for the Sturtian
474 glaciation having extended to equatorial latitudes (Macdonald et al., 2010).

475 There are more published models that show snapshots and publish rotation parameters
476 associated with given time intervals such as the Rodinia model of Li et al. (2008) and the
477 Mesoproterozoic model of Pisarevsky et al. (2014), but did not publish parameters for a
478 continuous model. The position for Laurentia implied by the Euler poles given for the model
479 snapshots of these studies are shown in Figure 5 and can be compared to the compiled record.
480 The compilation also shows the continuous implied position of Laurentia from the late
481 Mesoproterozoic into the early Paleozoic from the model of (Li et al., 2013; while the model

482 parameters were not published with that study they have now been made available by the
483 authors).

484 **3.7 The record implies plate tectonics throughout the Proterozoic**

485 There is strong evidence both in Laurentia's geological and paleomagnetic record for differential
486 plate tectonic motion between 2.2 and 1.8 Ga. The continued history of accretionary orogenesis
487 and the evaluation of Laurentia's pole path in comparison to other continents from 1.8 Ga onward
488 supports the continual operation of plate tectonics throughout the rest of the Proterozoic and
489 Phanerozoic as well. While this evidence fits with the majority of interpretations of the timing of
490 initiation of modern-style plate tectonics (see summary in Korenaga, 2013), there continue to be
491 arguments proposing that a stagnant lid persisted through the Mesoproterozoic Era (1.6 to 1.0
492 Ga) and into the Neoproterozoic with plate tectonics not initiating until ca. 0.8 Ga (Hamilton,
493 2011; Stern and Miller, 2018). These arguments rest largely on the relative lack of Proterozoic
494 low-temperature high-pressure metamorphic rocks such as blueschists that form in subduction
495 zones (Stern et al., 2013). An alternative interpretation for this lack of blueschists in the
496 Proterozoic is that such a shift in metamorphic regime is the predicted result of secular evolution
497 of mantle chemistry rather than a harbinger of the onset of plate tectonics (Palin and White,
498 2015). While this line of evidence is intriguing, to argue that there was not differential plate
499 tectonic motion in the Paleoproterozoic and Mesoproterozoic is to ignore a vast breadth and
500 depth of geological and paleomagnetic data. From a paleomagnetic perspective, there is strong
501 support for independent and differential motion of the Slave and Superior provinces as is
502 illustrated in Figure 4. From a geological perspective, the Trans-Hudson orogenic cycle, the
503 Grenville orogenic cycle, and the Appalachian orogenic cycle are all well-explained with a
504 mobilistic interpretation that includes phases of accretionary followed by collisional orogenesis
505 (Fig. 2). One could counter that this perspective results from a plate-tectonic-centric viewpoint
506 that lacks creativity to see the record as resulting from other processes than modern-style plate
507 tectonics. However, in addition to the broad geological record showing an amalgamation of
508 terranes as would be expected to arise through plate tectonics, there are also eclogites preserved
509 in the Trans-Hudson orogen that preserve evidence for high-pressure/low-temperature

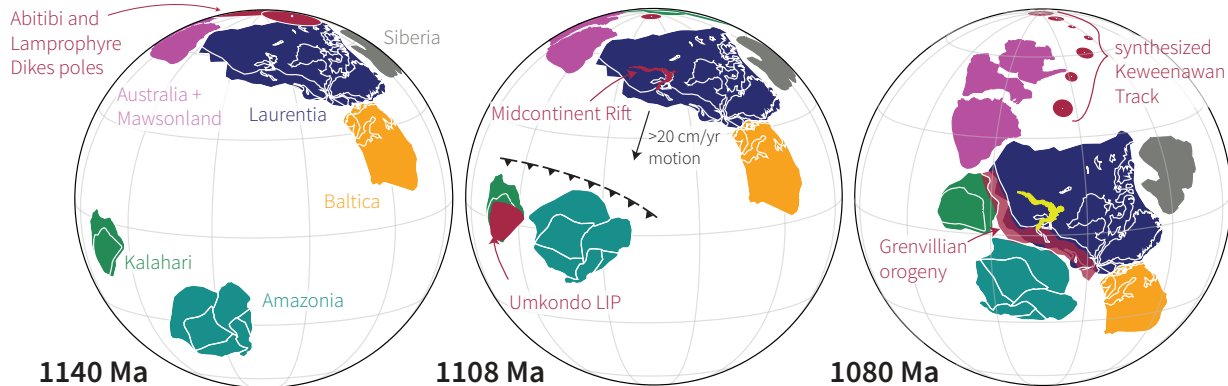


Figure 7. Paleogeographic reconstructions of Laurentia and other select Proterozoic continents leading up to Rodinia assembly in the late Mesoproterozoic modified from Swanson-Hysell et al. (2019). The record of paleomagnetic poles implies rapid motion which is consistent with the timing of collisional orogenesis associated with the Grenvillian orogeny.

metamorphic conditions ca. 1.8 Ga (Weller and St-Onge, 2017). Similar to the Himalayan orogen, these rocks are interpreted to be the result of deep continental subduction and exhumation associated with convergent plate tectonics (Weller and St-Onge, 2017). Outside of Laurentia, there are examples of eclogites with geochemical affinity to oceanic crust such as that documented in the ca. 1.9 Ga Ubendian Belt of the Congo craton (Boniface et al., 2012).

Another perspective on Proterozoic tectonics, is that the record is one of intermittent subduction (Silver and Behn, 2008; O'Neill et al., 2013). In such a model, there are extended intervals with a stagnant lid alternating with intervals of differential plate motion. In particular, it has been argued that the Mesoproterozoic Era (1.6 to 1.0 Ga) is an interval when Earth was in a stagnant regime (Silver and Behn, 2008; O'Neill et al., 2013). The accretionary history of Laurentia following the amalgamation of the Archean provinces is difficult to reconcile with such an interpretation (Figs. 1 and 2). An additional constraint comes from the paleomagnetic record and paleomagnetic poles supported with baked contact tests through the Mesoproterozoic. In a stagnant lid regime, there would not be sufficient heat flow across the core-mantle boundary to is necessary to sustain a geodynamo (Nimmo and Stevenson, 2000; Buffett, 2000). Baked contact tests indicate that, at the time of dike emplacement, there was an appreciable field such that both the cooling magma and the heated country rock in the vicinity of a dike were able to acquire a primary coherent magnetization direction. Additionally, since paleomagnetic poles are developed from many individual cooling units across a region, the similarity of the directions across an

529 igneous province indicates that the magnetizations were dominantly acquired from the
530 geomagnetic field rather than being influenced by local variable crustal magnetizations.
531 Therefore, the record supports the persistence of a geomagnetic field through the Paleoproterozoic
532 and Mesoproterozoic (Table 2) which implies active plate tectonics that enabled sufficient
533 core-mantle boundary heat flow to power the geodynamo. This interpretation of a significant
534 persistent geomagnetic field through much of the Proterozoic (with the potential exception of the
535 Ediacaran; Bono et al., 2019) is further bolstered by estimates of paleointensity obtained from
536 mafic dikes from Laurentia (e.g. Macouin et al., 2006) and elsewhere.

537 The record of these poles also show that there was progressive motion of Laurentia through the
538 Proterozoic (Figs. 5 and 6). Using data from Laurentia alone, however, it is difficult to ascertain
539 whether this motion is due to plate tectonic motion or rotation of the entire solid Earth through
540 true polar wander. True polar wander can lead to changing position relative to the spin axis even
541 with a stagnant lid. One interval when the Laurentian paleomagnetic record demands that some
542 of the motion is through differential plate tectonics is in the latest Mesoproterozoic. At that time,
543 the pole path is very well-resolved with many high-quality paleomagnetic poles between 1110 and
544 1070 Ma (Table 2; 3). The progression of the poles requires rotation about an Euler pole that is
545 distinct from a great circle path which would result if the motion were solely due to true polar
546 wander (Swanson-Hysell et al., 2019). These poles constrain rapid motion of Laurentia leading up
547 to collisional orogenesis associated with the Grenvillian orogeny as illustrated in Figure 7. These
548 data provide strong evidence for differential plate motion at the time and are inconsistent with a
549 stagnant lid. Rather the orogenic cycle of the Mesoproterozoic bears similarity with that of the
550 Paleozoic and reveals Laurentia to have been a central player in the building of amalgamated
551 continents associated with Rodinia and Pangea.

552 4 Conclusion

553 The paleogeographic record of Laurentia is rich in constraints through the Precambrian both in
554 terms of the geological and geochronological constraints on tectonism and the record of
555 paleomagnetic poles. As can be seen in the Chapters on Archean paleogeography (Salminen et al.,

556 this volume), Nuna (Elming et al., this volume) and Rodinia (Evans et al., this volume), these
557 constraints are at the center of paleogeographic models through the Precambrian and will
558 continue to be as the next generation of paleogeographic models are developed.

559 Acknowledgements

560 Many participants in the Nordic Paleomagnetism Workshop have contributed to the compilation
561 and evaluation of the pole list utilized herein. Particular acknowledgement goes to David Evans
562 for maintaining and distributing the compiled pole lists as well as additional efforts of Lauri
563 Pesonen in maintaining the Paleomagia database (Veikkolainen et al., 2014). GPlates, and in
564 particular the pyGPlates API, was utilized in this work (Müller et al., 2018). Figures were made
565 using Matplotlib (Hunter, 2007) in conjunction with cartopy (Met Office, 2010 - 2015) and
566 pmagpy (Tauxe et al., 2016) within an interactive Python environment (Pérez and Granger,
567 2007). This work was supported by NSF CAREER Grant EAR-1847277 awarded to N.L.S.-H.
568 The code, data, and reconstructions used in this paper are openly available in this repository:
569 https://github.com/Swanson-Hysell-Group/Laurentia_Paleogeography.

570 References

- 571 Abrahamsen, N. and Van Der Voo, R., 1987, Palaeomagnetism of middle Proterozoic (c. 1.25 Ga) dykes from central
572 North Greenland: Geophysical Journal International, v. 91, p. 597–611, doi:10.1111/j.1365-246x.1987.tb01660.x.
- 573 Abrajevitch, A. and Van der Voo, R., 2010, Incompatible Ediacaran paleomagnetic directions suggest an equatorial
574 geomagnetic dipole hypothesis: Earth and Planetary Science Letters, v. 293, p. 164–170.
- 575 Bates, M. P. and Halls, H. C., 1991, Broad-scale Proterozoic deformation of the central Superior Province revealed
576 by paleomagnetism of the 2.45 Ga Matachewan dyke swarm: Canadian Journal of Earth Sciences, v. 28, p.
577 1780–1796, doi:10.1139/e91-159.
- 578 Berman, R., Davis, A., and Pehrsson, S., 2007, Collisional Snowbird tectonic zone resurrected: Growth of Laurentia
579 during the 1.9 Ga accretionary phase of the Hudsonian orogeny: Geology, v. 35, p. 911–914,
580 doi:10.1130/G23771A.1.
- 581 Bickford, M., Van Schmus, W., Karlstrom, K., Mueller, P., and Kamenov, G., 2015,
582 Mesoproterozoic-trans-Laurentian magmatism: A synthesis of continent-wide age distributions, new SIMS U–Pb

- 583 ages, zircon saturation temperatures, and Hf and Nd isotopic compositions: Precambrian Research, v. 265, p.
584 286–312, doi:10.1016/j.precamres.2014.11.024.
- 585 Bond, G., Nickleson, P., and Kominz, M., 1984, Breakup of a supercontinent between 625 and 555 Ma: new
586 evidence and implications for continental histories: Earth and Planetary Science Letters, v. 70, p. 325–345,
587 doi:10.1016/0012-821X(84)90017-7.
- 588 Boniface, N., Schenk, V., and Appel, P., 2012, Paleoproterozoic eclogites of MORB-type chemistry and three
589 Proterozoic orogenic cycles in the Ubendian Belt (Tanzania): Evidence from monazite and zircon geochronology,
590 and geochemistry: Precambrian Research, v. 192–195, p. 16–33, doi:10.1016/j.precamres.2011.10.007.
- 591 Bono, R. K., Tarduno, J. A., Nimmo, F., and Cottrell, R. D., 2019, Young inner core inferred from Ediacaran
592 ultra-low geomagnetic field intensity: Nature Geoscience, v. 12, p. 143–147, doi:10.1038/s41561-018-0288-0.
- 593 Books, K., 1972, Paleomagnetism of some Lake Superior Keweenawan rocks: U.S. Geological Survey Professional
594 Paper, v. P 0760, p. 42.
- 595 Borradaile, G. and Middleton, R., 2006, Proterozoic paleomagnetism in the Nipigon Embayment of northern
596 Ontario: Pillar Lake Lava, Wawieg Troctolite and Gunflint Formation tuffs: Precambrian Research, v. 144, p.
597 69–91, doi:10.1016/j.precamres.2005.10.007.
- 598 Brown, L. L. and McEnroe, S. A., 2012, Paleomagnetism and magnetic mineralogy of Grenville metamorphic and
599 igneous rocks, Adirondack Highlands, USA: Precambrian Research, v. 212–213, p. 57–74,
600 doi:10.1016/j.precamres.2012.04.012.
- 601 Buchan, K., Mertanen, S., Park, R., Pesonen, L., Elming, S. A., Abrahamsen, N., and Bylund, G., 2000, Comparing
602 the drift of Laurentia and Baltica in the Proterozoic: the importance of key paleomagnetic poles:
603 Tectonophysics, v. 319, p. 167–198.
- 604 Buchan, K. L., LeCheminant, A. N., and van Breemen, O., 2009, Paleomagnetism and U–Pb geochronology of the
605 Lac de Gras diabase dyke swarm, Slave Province, Canada: implications for relative drift of Slave and Superior
606 provinces in the Paleoproterozoic: Canadian Journal of Earth Sciences, v. 46, p. 361–379, doi:10.1139/e09-026.
- 607 Buchan, K. L., LeCheminant, A. N., and van Breemen, O., 2012, Malley diabase dykes of the Slave craton,
608 Canadian Shield: U–Pb age, paleomagnetism, and implications for continental reconstructions in the early
609 Paleoproterozoic: Canadian Journal of Earth Sciences, v. 49, p. 435–454, doi:10.1139/e11-061.
- 610 Buchan, K. L., Mitchell, R. N., Bleeker, W., Hamilton, M. A., and LeCheminant, A. N., 2016, Paleomagnetism of
611 ca. 2.13–2.11 Ga Indin and ca. 1.885 Ga Ghost dyke swarms of the Slave craton: Implications for the Slave
612 craton APW path and relative drift of Slave, Superior and Siberian cratons in the Paleoproterozoic: Precambrian
613 Research, v. 275, p. 151–175, doi:10.1016/j.precamres.2016.01.012.

- 614 Buchan, K. L., Mortensen, J. K., and Card, K. D., 1993, Northeast-trending early Proterozoic dykes of southern
615 Superior Province: multiple episodes of emplacement recognized from integrated paleomagnetism and U–Pb
616 geochronology: Canadian Journal of Earth Sciences, v. 30, p. 1286–1296, doi:10.1139/e93-110.
- 617 Buffett, B. A., 2000, Earth’s core and the geodynamo: Science, v. 288, p. 2007–2012.
- 618 Burton, W. C. and Southworth, S., 2010, A model for Iapetan rifting of Laurentia based on Neoproterozoic dikes
619 and related rocks: From Rodinia to Pangea: The Lithotectonic Record of the Appalachian Region, p. 455–476,
620 doi:10.1130/2010.1206(20).
- 621 Cannon, W. F., 1992, The Midcontinent rift in the Lake Superior region with emphasis on its geodynamic
622 evolution: Tectonophysics, v. 213, p. 41–48, doi:10.1016/0040-1951(92)90250-A.
- 623 Casquet, C., Dahlquist, J. A., Verdecchia, S. O., Baldo, E. G., Galindo, C., Rapela, C. W., Pankhurst, R. J.,
624 Morales, M. M., Murra, J. A., and Mark Fanning, C., 2018, Review of the Cambrian Pampean orogeny of
625 Argentina; a displaced orogen formerly attached to the Saldania Belt of South Africa?: Earth-Science Reviews, v.
626 177, p. 209–225, doi:10.1016/j.earscirev.2017.11.013.
- 627 Condit, C. B., Mahan, K. H., Ault, A. K., and Flowers, R. M., 2015, Foreland-directed propagation of high-grade
628 tectonism in the deep roots of a Paleoproterozoic collisional orogen, SW Montana, USA: Lithosphere, p. L460.1,
629 doi:10.1130/l460.1.
- 630 Corrigan, D., Pehrsson, S., Wodicka, N., and de Kemp, E., 2009, The Palaeoproterozoic Trans-Hudson Orogen: a
631 prototype of modern accretionary processes: Geological Society, London, Special Publications, v. 327, p.
632 457–479, doi:10.1144/sp327.19.
- 633 Dahl, P. S., Holm, D. K., Gardner, E. T., Hubacher, F. A., and Foland, K. A., 1999, New constraints on the timing
634 of Early Proterozoic tectonism in the Black Hills (South Dakota), with implications for docking of the Wyoming
635 province with Laurentia: Geological Society of America Bulletin, v. 111, p. 1335–1349,
636 doi:10.1130/0016-7606(1999)111<1335:ncotto>2.3.co;2.
- 637 Denyszyn, S. W., Davis, D. W., and Halls, H. C., 2009a, Paleomagnetism and U–Pb geochronology of the Clarence
638 Head dykes, Arctic Canada: orthogonal emplacement of mafic dykes in a large igneous province: Canadian
639 Journal of Earth Sciences, v. 46, p. 155–167, doi:10.1139/E09-011.
- 640 Denyszyn, S. W., Halls, H. C., Davis, D. W., and Evans, D. A. D., 2009b, Paleomagnetism and U–Pb geochronology
641 of Franklin dykes in High Arctic Canada and Greenland: a revised age and paleomagnetic pole constraining block
642 rotations in the Nares Strait region: Canadian Journal of Earth Sciences, v. 46, p. 689–705, doi:10.1139/E09-042.
- 643 Dickerson, P. W. and Keller, M., 1998, The Argentine Precordillera: its odyssey from the Laurentian Ouachita
644 margin towards the Sierras Pampeanas of Gondwana: Geological Society, London, Special Publications, v. 142,
645 p. 85–105, doi:10.1144/gsl.sp.1998.142.01.05.

- 646 Donadini, F., Pesonen, L. J., Korhonen, K., Deutsch, A., and Harlan, S. S., 2011, Paleomagnetism and
647 paleointensity of the 1.1 Ga old diabase sheets from central Arizona: *Geophysica*, v. 47, p. 3–30.
- 648 Elming, S. Å., D’Agrella-Filho, M. S., Page, L. M., Tohver, E., Trindade, R. I. F., Pacca, I. I. G., Geraldes, M. C.,
649 and Teixeira, W., 2009, A palaeomagnetic and 40Ar/39Ar study of late precambrian sills in the SW part of the
650 Amazonian craton: *Amazonia in the Rodinia reconstruction: Geophysical Journal International*, v. 178, p.
651 106–122.
- 652 Elston, D. P., Enkin, R. J., Baker, J., and Kisilevsky, D. K., 2002, Tightening the Belt: Paleomagnetic-stratigraphic
653 constraints on deposition, correlation, and deformation of the Middle Proterozoic (ca. 1.4 Ga) Belt-Purcell
654 Supergroup, United States and Canada: *GSA Bulletin*, v. 114, p. 619–638,
655 doi:10.1130/0016-7606(2002)114<0619:TTBPSC>2.0.CO;2.
- 656 Emslie, R. F., Irving, E., and Park, J. K., 1976, Further paleomagnetic results from the Michikamau Intrusion,
657 Labrador: *Canadian Journal of Earth Sciences*, v. 13, p. 1052–1057, doi:10.1139/e76-108.
- 658 Ernst, R. and Buchan, K., 1993, Paleomagnetism of the Abitibi dike swarm, southern Superior Province, and
659 implications for the Logan Loop: *Canadian Journal of Earth Science*, v. 30, p. 1886–1897, doi:10.1139/e93-167.
- 660 Evans, D. and Halls, H., 2010, Restoring Proterozoic deformation within the Superior craton: *Precambrian
661 Research*, v. 183, p. 474 – 489, doi:10.1016/j.precamres.2010.02.007.
- 662 Evans, M. E. and Bingham, D. K., 1973, Paleomagnetism of the Precambrian Martin Formation, Saskatchewan:
663 *Canadian Journal of Earth Sciences*, v. 10, p. 1485–1493, doi:10.1139/e73-141.
- 664 Evans, M. E. and Hoye, G. S., 1981, Paleomagnetic results from the lower proterozoic rocks of Great Slave Lake and
665 Bathurst Inlet areas, Northwest Territories: *In Proterozoic Basins of Canada*; Geological Survey of Canada,
666 Paper 81-10, Natural Resources Canada/ESS/Scientific and Technical Publishing Services, doi:10.4095/109374.
- 667 Eyster, A., Weiss, B. P., Karlstrom, K., and Macdonald, F. A., 2019, Paleomagnetism of the Chuar Group and
668 evaluation of the late Tonian Laurentian apparent polar wander path with implications for the makeup and
669 breakup of Rodinia: *GSA Bulletin*, doi:10.1130/b32012.1.
- 670 Fahrig, W. and Bridgwater, D., 1976, Late Archean-early Proterozoic paleomagnetic pole positions from west
671 Greenland: *In Windley, B., ed., Early History of the Earth*, Wiley, p. 427–442.
- 672 Fahrig, W. F. and Jones, D. L., 1976, The paleomagnetism of the Helikian Mistastin pluton, Labrador, Canada:
673 *Canadian Journal of Earth Sciences*, v. 13, p. 832–837, doi:10.1139/e76-086.
- 674 Fairchild, L. M., Swanson-Hysell, N. L., Ramezani, J., Sprain, C. J., and Bowring, S. A., 2017, The end of
675 Midcontinent Rift magmatism and the paleogeography of Laurentia: *Lithosphere*, v. 9, p. 117–133,
676 doi:10.1130/L580.1.

- 677 Gala, M. G., Symons, D. T. A., and Palmer, H. C., 1995, Paleomagnetism of the Jan Lake Granite, Trans-Hudson
678 Orogen: Saskatchewan Geological Survey Summary of Investigations, v. 95-4.
- 679 Halls, H., 1974, A paleomagnetic reversal in the Osler Volcanic Group, northern Lake Superior: Canadian Journal
680 of Earth Science, v. 11, p. 1200–1207, doi:10.1139/e74-113.
- 681 Halls, H. C., 2015, Paleomagnetic evidence for ~4000 km of crustal shortening across the 1 Ga Grenville orogen of
682 North America: Geology, v. 43, p. 1051–1054, doi:10.1130/G37188.1.
- 683 Halls, H. C., Davis, D. W., Stott, G. M., Ernst, R. E., and Hamilton, M. A., 2008, The Paleoproterozoic Marathon
684 Large Igneous Province: New evidence for a 2.1 Ga long-lived mantle plume event along the southern margin of
685 the North American Superior Province: Precambrian Research, v. 162, p. 327–353,
686 doi:10.1016/j.precamres.2007.10.009.
- 687 Halls, H. C., Hamilton, M. A., and Denyszyn, S. W., 2011, The Melville Bugt Dyke Swarm of Greenland: A
688 Connection to the 1.5-1.6 Ga Fennoscandian Rapakivi Granite Province?, Springer Berlin Heidelberg, p. 509–535:
689 doi:10.1007/978-3-642-12496-9{_\}27.
- 690 Halls, H. C. and Hanes, J. A., 1999, Paleomagnetism, anisotropy of magnetic susceptibility, and argon–argon
691 geochronology of the Clearwater anorthosite, Saskatchewan, Canada: Tectonophysics, v. 312, p. 235–248,
692 doi:10.1016/s0040-1951(99)00166-3.
- 693 Halls, H. C., Lovette, A., Hamilton, M., and Söderlund, U., 2015, A paleomagnetic and u–pb geochronology study
694 of the western end of the grenville dyke swarm: Rapid changes in paleomagnetic field direction at ca.
695 585 ma related to polarity reversals?: Precambrian Research, v. 257, p. 137–166,
696 doi:<http://dx.doi.org/10.1016/j.precamres.2014.11.029>.
- 697 Halverson, G. P., Porter, S. M., and Gibson, T. M., 2018, Dating the late Proterozoic stratigraphic record:
698 Emerging Topics in Life Sciences, v. 2, p. 137–147, doi:10.1042/etls20170167.
- 699 Hamilton, W. B., 2011, Plate tectonics began in Neoproterozoic time, and plumes from deep mantle have never
700 operated: Lithos, v. 123, p. 1–20, doi:10.1016/j.lithos.2010.12.007.
- 701 Harlan, S., 1993, Paleomagnetism of Middle Proterozoic diabase sheets from central Arizona: Canadian Journal of
702 Earth Science, v. 30, p. 1415–1426.
- 703 Harlan, S., Geissman, J., and Snee, L., 1997, Paleomagnetic and $^{40}\text{Ar}/^{39}\text{Ar}$ geochronologic data from late
704 Proterozoic mafic dykes and sills, Montana and Wyoming: USGS Professional Paper, v. 1580, p. 16.
- 705 Harlan, S. S. and Geissman, J. W., 1998, Paleomagnetism of the middle Proterozoic Electra Lake Gabbro, Needle
706 Mountains, southwestern Colorado: Journal of Geophysical Research: Solid Earth, v. 103, p. 15,497–15,507,
707 doi:10.1029/98jb01350.

- 708 Harlan, S. S., Geissman, J. W., and Snee, L. W., 2008, Paleomagnetism of Proterozoic mafic dikes from the Tobacco
709 Root Mountains, southwest Montana: *Precambrian Research*, v. 163, p. 239–264.
- 710 Harlan, S. S., Snee, L. W., Geissman, J. W., and Brearley, A. J., 1994, Paleomagnetism of the middle proterozoic
711 laramie anorthosite complex and sherman granite, southern laramie range, wyoming and colorado: *Journal of*
712 *Geophysical Research: Solid Earth*, v. 99, p. 17,997–18,020, doi:10.1029/94jb00580.
- 713 Henry, S., Mauk, F., and Van der Voo, R., 1977, Paleomagnetism of the upper Keweenawan sediments: Nonesuch
714 Shale and Freda Sandstone: *Canadian Journal of Earth Science*, v. 14, p. 1128–1138, doi:10.1139/e77-103.
- 715 Hildebrand, R. S., Hoffman, P. F., and Bowring, S. A., 2009, The Calderian orogeny in Wopmay orogen (1.9 Ga),
716 northwestern Canadian Shield: *Geological Society of America Bulletin*, v. 122, p. 794–814, doi:10.1130/B26521.1.
- 717 Hnat, J. S., van der Pluijm, B. A., and Van der Voo, R., 2006, Primary curvature in the Mid-Continent Rift:
718 Paleomagnetism of the Portage Lake Volcanics (northern Michigan, USA): *Tectonophysics*, v. 425, p. 71–82,
719 doi:10.1016/j.tecto.2006.07.006.
- 720 Hoffman, P., 1991, Did the breakout of Laurentia turn Gondwana inside out?: *Science*, v. 252, p. 1409–1412.
- 721 Hoffman, P. F., 1988, United plates of America, the birth of a craton: Early Proterozoic assembly and growth of
722 Laurentia: *Annual Review of Earth and Planetary Sciences*, v. 16, p. 543–603,
723 doi:10.1146/annurev.ea.16.050188.002551.
- 724 Hoffman, P. F., 1989, Speculations on Laurentia's first gigayear (2.0 to 1.0 Ga): *Geology*, v. 17, p. 135–138,
725 doi:10.1130/0091-7613(1989)017<0135:SOLSFG>2.3.CO;2.
- 726 Hoffman, P. F., Halverson, G. P., Domack, E. W., Maloof, A. C., Swanson-Hysell, N. L., and Cox, G. M., 2012,
727 Cryogenian glaciations on the southern tropical paleomargin of Laurentia (NE Svalbard and East Greenland),
728 and a primary origin for the upper Russøya (Islay) carbon isotope excursion: *Precambrian Research*, v. 206–207,
729 p. 137–158, doi:10.1016/j.precamres.2012.02.018.
- 730 Holm, D. K., Van Schmus, W. R., MacNeill, L. C., Boerboom, T. J., Schweitzer, D., and Schneider, D., 2005, U-Pb
731 zircon geochronology of Paleoproterozoic plutons from the northern midcontinent, USA: Evidence for subduction
732 flip and continued convergence after geon 18 Penokean orogenesis: *Geological Society of America Bulletin*, v. 117,
733 p. 259, doi:10.1130/b25395.1.
- 734 Hrncir, J., Karlstrom, K., and Dahl, P., 2017, Wyoming on the run—Toward final Paleoproterozoic assembly of
735 Laurentia: COMMENT: *Geology*, v. 45, p. e411–e411, doi:10.1130/g38826c.1.
- 736 Hunter, J. D., 2007, Matplotlib: A 2D graphics environment: *Computing in Science & Engineering*, v. 9, p. 90–95,
737 doi:10.1109/MCSE.2007.55.

- 738 Irving, E., 2004, Early Proterozoic geomagnetic field in western Laurentia: implications for paleolatitudes, local
739 rotations and stratigraphy: *Precambrian Research*, v. 129, p. 251–270, doi:10.1016/j.precamres.2003.10.002.
- 740 Irving, E. and McGlynn, J. C., 1979, Palaeomagnetism in the Coronation Geosyncline and arrangement of
741 continents in the middle Proterozoic: *Geophysical Journal International*, v. 58, p. 309–336,
742 doi:10.1111/j.1365-246X.1979.tb01027.x.
- 743 Irving, E. and Park, J. K., 1972, Hairpins and superintervals: *Canadian Journal of Earth Sciences*, v. 9, p.
744 1318–1324, doi:10.1139/e72-115.
- 745 Jones, J. V., Daniel, C. G., and Doe, M. F., 2015, Tectonic and sedimentary linkages between the Belt-Purcell basin
746 and southwestern Laurentia during the Mesoproterozoic, ca. 1.60–1.40 Ga: *Lithosphere*, v. 7, p. 465–472,
747 doi:10.1130/l438.1.
- 748 Karlstrom, K. E., Ahall, K.-I., Harlan, S. S., Williams, M. L., McLelland, J., and Geissman, J. W., 2001, Long-lived
749 (1.8-1.0 Ga) convergent orogen in southern Laurentia, its extensions to Australia and Baltica, and implications
750 for refining Rodinia: *Precambrian Research*, v. 111, p. 5–30, doi:10.1016/S0301-9268(01)00154-1.
- 751 Karlstrom, K. E. and Bowring, S. A., 1988, Early Proterozoic assembly of tectonostratigraphic terranes in
752 southwestern North America: *The Journal of Geology*, v. 96, p. 561–576, doi:10.1086/629252.
- 753 Kean, W., Williams, I., and Feeney, J., 1997, Magnetism of the Keweenawan age Chengwatana lava flows,
754 northwest Wisconsin: *Geophysical Research Letters*, v. 24, p. 1523–1526, doi:10.1029/97gl00993.
- 755 Kilian, T. M., Bleeker, W., Chamberlain, K., Evans, D. A. D., and Cousens, B., 2015, Palaeomagnetism,
756 geochronology and geochemistry of the Palaeoproterozoic Rabbit Creek and Powder River dyke swarms:
757 implications for Wyoming in supercraton Superia: *Geological Society, London, Special Publications*, v. 424, p.
758 15–45, doi:10.1144/sp424.7.
- 759 Kilian, T. M., Chamberlain, K. R., Evans, D. A., Bleeker, W., and Cousens, B. L., 2016, Wyoming on the
760 run—Toward final Paleoproterozoic assembly of Laurentia: *Geology*, v. 44, p. 863–866, doi:10.1130/g38042.1.
- 761 Korenaga, J., 2013, Initiation and evolution of plate tectonics on earth: Theories and observations: *Annual Review*
762 of Earth and Planetary Sciences, v. 41, p. 117–151, doi:10.1146/annurev-earth-050212-124208.
- 763 Kulakov, E. V., Smirnov, A. V., and Diehl, J. F., 2013, Paleomagnetism of ~1.09 Ga Lake Shore Traps (Keweenaw
764 Peninsula, Michigan): new results and implications: *Canadian Journal of Earth Sciences*, v. 50, p. 1085–1096,
765 doi:10.1139/cjes-2013-0003.
- 766 Levy, M. and Christie-Blick, N., Nicholas, 1991, Tectonic subsidence of the early Paleozoic passive continental
767 margin in eastern California and southern Nevada: *Geological Society of America Bulletin*, v. 103, p. 1590–1606,
768 doi:10.1130/0016-7606(1991)103<1590:tsotep>2.3.co;2.

- 769 Li, Z.-X., Evans, D. A. D., and Halverson, G., 2013, Neoproterozoic glaciations in a revised global palaeogeography
770 from the breakup of Rodinia to the assembly of Gondwanaland: *Sedimentary Geology*, v. 294, p. 219–232,
771 doi:10.1016/j.sedgeo.2013.05.016.
- 772 Li, Z. X. et al., 2008, Assembly, configuration, and break-up history of Rodinia: A synthesis: *Precambrian*
773 *Research*, v. 160, p. 179–210, doi:10.1016/j.precamres.2007.04.021.
- 774 Macdonald, F., Halverson, G., Strauss, J., Smith, E., Cox, G., Sperling, E., and Roots, C., 2012, Early
775 Neoproterozoic basin formation in Yukon, Canada: Implications for the make-up and break-up of Rodinia:
776 *Geoscience Canada*, v. 39.
- 777 Macdonald, F. A., Schmitz, M. D., Crowley, J. L., Roots, C. F., Jones, D. S., Maloof, A. C., Strauss, J. V., Cohen,
778 P. A., Johnston, D. T., and Schrag, D. P., 2010, Calibrating the Cryogenian: *Science*, v. 327, p. 1241–1243,
779 doi:10.1126/science.1183325.
- 780 Macouin, M., Valet, J. P., Besse, J., and Ernst, R. E., 2006, Absolute paleointensity at 1.27 Ga from the Mackenzie
781 dyke swarm (Canada): *Geochem. Geophys. Geosyst.*, v. 7, p. 10.1029/2005GC000960.
- 782 Maloof, A., Halverson, G., Kirschvink, J., Schrag, D., Weiss, B., and Hoffman, P., 2006, Combined paleomagnetic,
783 isotopic and stratigraphic evidence for true polar wander from the Neoproterozoic Akademikerbreen Group,
784 Svalbard, Norway: *Geological Society of America Bulletin*, v. 118, p. 1099–1124, doi:10.1130/B25892.1.
- 785 Marcussen, C. and Abrahamsen, N., 1983, Palaeomagnetism of the Proterozoic Zig-Zag Dal Basalt and the
786 Midsommerso Dolerites, eastern North Greenland: *Geophysical Journal International*, v. 73, p. 367–387,
787 doi:10.1111/j.1365-246x.1983.tb03321.x.
- 788 Martin, E. L., Collins, W. J., and Spencer, C. J., 2019, Laurentian origin of the Cuyania suspect terrane, western
789 Argentina, confirmed by Hf isotopes in zircon: *GSA Bulletin*, doi:10.1130/b35150.1.
- 790 McCausland, P. J. A., Hankard, F., Van der Voo, R., and Hall, C. M., 2011, Ediacaran paleogeography of
791 Laurentia: Paleomagnetism and 40Ar-39Ar geochronology of the 583 Ma Baie des Moutons syenite, Quebec:
792 *Precambrian Research*, v. 187, p. 58–78, doi:10.1016/j.precamres.2011.02.004.
- 793 McCausland, P. J. A., Van der Voo, R., and Hall, C. M., 2007, Circum-Iapetus paleogeography of the
794 Precambrian–Cambrian transition with a new paleomagnetic constraint from Laurentia: *Precambrian Research*,
795 v. 156, p. 125–152, doi:10.1016/j.precamres.2007.03.004.
- 796 McFarlane, C. R., 2015, A geochronological framework for sedimentation and Mesoproterozoic tectono-magmatic
797 activity in lower Belt–Purcell rocks exposed west of Kimberley, British Columbia: *Canadian Journal of Earth*
798 *Sciences*, v. 52, p. 444–465, doi:10.1139/cjes-2014-0215.

- 799 McGlynn, J. C., Hanson, G. N., Irving, E., and Park, J. K., 1974, Paleomagnetism and age of Nonacho Group
800 sandstones and associated Sparrow dikes, District of Mackenzie: Canadian Journal of Earth Sciences, v. 11, p.
801 30–42, doi:10.1139/e74-003.
- 802 McLelland, J. M., Selleck, B. W., and Bickford, M., 2010, Review of the Proterozoic evolution of the Grenville
803 Province, its Adirondack outlier, and the Mesoproterozoic inliers of the Appalachians: From Rodinia to Pangea:
804 The Lithotectonic Record of the Appalachian Region, p. 21–49, doi:10.1130/2010.1206(02).
- 805 McLelland, J. M., Selleck, B. W., and Bickford, M. E., 2013, Tectonic evolution of the Adirondack Mountains and
806 Grenville Orogen inliers within the USA: Geoscience Canada, v. 40, p. 318, doi:10.12789/geocanj.2013.40.022.
- 807 McMechan, M. E. and Price, R. A., 1982, Superimposed low-grade metamorphism in the Mount Fisher area,
808 southeastern British Columbia—implications for the East Kootenay orogeny: Canadian Journal of Earth
809 Sciences, v. 19, p. 476–489, doi:10.1139/e82-039.
- 810 Meert, J., der Voo, R. V., and Payne, T., 1994, Paleomagnetism of the Catoctin volcanic province: a new
811 Vendian-Cambrian apparent polar wander path for North America: Journal of Geophysical Research, v. 99, p.
812 4625–4641.
- 813 Meert, J. G. and Stuckey, W., 2002, Revisiting the paleomagnetism of the 1.476 Ga St. Francois Mountains igneous
814 province, Missouri: Tectonics, v. 21, doi:10.1029/2000tc001265.
- 815 Meredith, A. S., Collins, A. S., Williams, S. E., Pisarevsky, S., Foden, J. D., Archibald, D. B., Blades, M. L., Alessio,
816 B. L., Armistead, S., Plavsa, D., and et al., 2017, A full-plate global reconstruction of the Neoproterozoic:
817 Gondwana Research, v. 50, p. 84–134, doi:10.1016/j.gr.2017.04.001.
- 818 Met Office, 2010 - 2015, Cartopy: a cartographic python library with a matplotlib interface: Exeter, Devon, URL
819 <http://scitools.org.uk/cartopy>.
- 820 Middleton, R. S., Borradaile, G. J., Baker, D., and Lucas, K., 2004, Proterozoic diabase sills of northern Ontario:
821 Magnetic properties and history: Journal of Geophysical Research: Solid Earth, v. 109,
822 doi:10.1029/2003jb002581.
- 823 Mitchell, R. N., Bleeker, W., van Breemen, O., Lecheminant, T. N., Peng, P., Nilsson, M. K. M., and Evans, D.
824 A. D., 2014, Plate tectonics before 2.0 Ga: Evidence from paleomagnetism of cratons within supercontinent
825 Nuna: American Journal of Science, v. 314, p. 878–894, doi:10.2475/04.2014.03.
- 826 Mitchell, R. N., Hoffman, P. F., and Evans, D. A. D., 2010, Coronation loop resurrected: Oscillatory apparent polar
827 wander of orosirian (2.05–1.8†ga) paleomagnetic poles from slave craton: Precambrian Research, v. 179, p.
828 121–134.
- 829 Mitchell, R. N., Kilian, T. M., and Evans, D. A. D., 2012, Supercontinent cycles and the calculation of absolute
830 palaeolongitude in deep time: Nature, v. 482, p. 208–211, doi:10.1038/nature10800.

- 831 Müller, R. D., Cannon, J., Qin, X., Watson, R. J., Gurnis, M., Williams, S., Pfaffelmoser, T., Seton, M., Russell, S.
832 H. J., and Zahirovic, S., 2018, GPlates: Building a virtual earth through deep time: Geochemistry, Geophysics,
833 Geosystems, v. 19, p. 2243–2261, doi:10.1029/2018gc007584.
- 834 Murthy, G., Gower, C., Tubett, M., and Patzold, R., 1992, Paleomagnetism of Eocambrian Long Range dykes and
835 Double Mer Formation from Labrador, Canada: Canadian Journal of Earth Sciences, v. 29, p. 1224–1234,
836 doi:10.1139/e92-098.
- 837 Murthy, G. S., 1978, Paleomagnetic results from the Nain anorthosite and their tectonic implications: Canadian
838 Journal of Earth Sciences, v. 15, p. 516–525, doi:10.1139/e78-058.
- 839 Nesheim, T. O., Vervoort, J. D., McClelland, W. C., Gilotti, J. A., and Lang, H. M., 2012, Mesoproterozoic
840 syntectonic garnet within Belt Supergroup metamorphic tectonites: Evidence of Grenville-age metamorphism
841 and deformation along northwest Laurentia: Lithos, v. 134–135, p. 91–107, doi:10.1016/j.lithos.2011.12.008.
- 842 Nimmo, F. and Stevenson, D. J., 2000, Influence of early plate tectonics on the thermal evolution and magnetic
843 field of Mars: Journal of Geophysical Research: Planets, v. 105, p. 11,969–11,979, doi:10.1029/1999je001216.
- 844 O'Neill, C., Lenardic, A., and Condie, K. C., 2013, Earth's punctuated tectonic evolution: cause and effect:
845 Geological Society, London, Special Publications, v. 389, p. 17–40, doi:10.1144/sp389.4.
- 846 Palin, R. M. and White, R. W., 2015, Emergence of blueschists on Earth linked to secular changes in oceanic crust
847 composition: Nature Geoscience, v. 9, p. 60–64, doi:10.1038/ngeo2605.
- 848 Palmer, H., 1970, Paleomagnetism and correlation of some Middle Keweenawan rocks, Lake Superior: Canadian
849 Journal of Earth Science, v. 7, p. 1410–1436, doi:10.1139/e70-136.
- 850 Palmer, H. C., Merz, B. A., and Hayatsu, A., 1977, The Sudbury dikes of the Grenville Front region:
851 paleomagnetism, petrochemistry, and K–Ar age studies: Canadian Journal of Earth Sciences, v. 14, p. 1867–1887.
- 852 Park, J. K., Irving, E., and Donaldson, J. A., 1973, Paleomagnetism of the Precambrian Dubawnt Group:
853 Geological Society of America Bulletin, v. 84, p. 859, doi:10.1130/0016-7606(1973)84<859:potpdg>2.0.co;2.
- 854 Pehrsson, S. J., Eglington, B. M., Evans, D. A. D., Huston, D., and Reddy, S. M., 2015, Metallogeny and its link to
855 orogenic style during the Nuna supercontinent cycle: Geological Society, London, Special Publications, v. 424,
856 doi:10.1144/SP424.5.
- 857 Pérez, F. and Granger, B. E., 2007, IPython: a system for interactive scientific computing: Computing in Science
858 and Engineering, v. 9, p. 21–29, doi:10.1109/MCSE.2007.53.
- 859 Pesonen, L., 1979, Paleomagnetism of late Precambrian Keweenawan igneous and baked contact rocks from
860 Thunder Bay district, northern Lake Superior: Bulletin of the Geological Society of Finland, v. 51, p. 27–44.

- 861 Pesonen, L. J. and Halls, H., 1979, The paleomagnetism of Keweenawan dikes from Baraga and Marquette
862 Counties, northern Michigan: Canadian Journal of Earth Science, v. 16, p. 2136–2149, doi:10.1139/e79-201.
- 863 Piispa, E. J., Smirnov, A. V., Pesonen, L. J., and Mitchell, R. H., 2018, Paleomagnetism and geochemistry of
864 1144-ma lamprophyre dikes, Northwestern Ontario: Implications for the North American polar wander and plate
865 velocities: Journal of Geophysical Research: Solid Earth, doi:10.1029/2018jb015992.
- 866 Piper, J., 1992, The palaeomagnetism of major (Middle Proterozoic) igneous complexes, South Greenland and the
867 Gardar apparent polar wander track: Precambrian Research, v. 54, p. 153 – 172,
868 doi:10.1016/0301-9268(92)90068-Y.
- 869 Piper, J. and Stearn, J., 1977, Palaeomagnetism of the dyke swarms of the Gardar Igneous Province, south
870 Greenland: Physics of the Earth and Planetary Interiors, v. 14, p. 345–358, doi:10.1016/0031-9201(77)90167-4.
- 871 Piper, J. D. A., 1977, Palaeomagnetism of the giant dykes of Tugtutoq and Narssaq Gabbro, Gardar Igneous
872 Province, South Greenland: Bull. Geol. Soc. Den, v. 26, p. 85–94.
- 873 Pisarevsky, S. A., Elming, S.-Å., Pesonen, L. J., and Li, Z.-X., 2014, Mesoproterozoic paleogeography:
874 Supercontinent and beyond: Precambrian Research, v. 244, p. 207–225, doi:10.1016/j.precamres.2013.05.014.
- 875 Pullaiah, G. and Irving, E., 1975, Paleomagnetism of the contact aureole and late dikes of the Otto stock, Ontario,
876 and its application to early proterozoic apparent polar wandering: Canadian Journal of Earth Sciences, v. 12, p.
877 1609–1618, doi:10.1139/e75-143.
- 878 Rapalini, A. E., 2018, The assembly of western Gondwana: Reconstruction based on paleomagnetic data: Geology
879 of Southwest Gondwana, p. 3–18, doi:10.1007/978-3-319-68920-3_1.
- 880 Redden, J., Peterman, Z., Zartman, R., and De-Witt, E., 1990, U-Th-Pb geochronology and preliminary
881 interpretation of Precambrian tectonic events in the Black Hills, South Dakota: *In* The Early Proterozoic
882 Trans-Hudson Orogen, Geological Association of Canada Special Paper 37, p. 229–251.
- 883 Rivers, T., 2008, Assembly and preservation of lower, mid, and upper orogenic crust in the Grenville
884 Province—implications for the evolution of large hot long-duration orogens: Precambrian Research, v. 167, p.
885 237–259, doi:10.1016/j.precamres.2008.08.005.
- 886 Robert, B., Besse, J., Blein, O., Greff-Lefftz, M., Baudin, T., Lopes, F., Meslouh, S., and Belbadaoui, M., 2017,
887 Constraints on the ediacaran inertial interchange true polar wander hypothesis: A new paleomagnetic study in
888 morocco (west african craton): Precambrian Research, v. 295, p. 90–116, doi:10.1016/j.precamres.2017.04.010.
- 889 Robertson, W. and Fahrig, W., 1971, The great Logan Loop - the polar wandering path from Canadian shield rocks
890 during the Neohelikian era: Canadian Journal of Earth Science, v. 8, p. 1355–1372, doi:10.1139/e71-125.

- 891 Roest, W. R. and Srivastava, S. P., 1989, Sea-floor spreading in the labrador sea: A new reconstruction: Geology,
892 v. 17, p. 1000, doi:10.1130/0091-7613(1989)017<1000:sfsitl>2.3.co;2.
- 893 Rooney, A. D., Austermann, J., Smith, E. F., Li, Y., Selby, D., Dehler, C. M., Schmitz, M. D., Karlstrom, K. E.,
894 and Macdonald, F. A., 2017, Coupled Re-Os and U-Pb geochronology of the Tonian Chuar Group, Grand
895 Canyon: GSA Bulletin, doi:10.1130/b31768.1.
- 896 Ross, G. M., 1991, Tectonic setting of the Windermere Supergroup revisited: Geology, v. 19, p. 1125,
897 doi:10.1130/0091-7613(1991)019<1125:tsotws>2.3.co;2.
- 898 Schmidt, P. W., 1980, Paleomagnetism of igneous rocks from the Belcher Islands, Northwest Territories, Canada:
899 Canadian Journal of Earth Sciences, v. 17, p. 807–822, doi:10.1139/e80-081.
- 900 Schulz, K. J. and Cannon, W. F., 2007, The Penokean orogeny in the Lake Superior region: Precambrian Research,
901 v. 157, p. 4–25, doi:10.1016/j.precamres.2007.02.022.
- 902 Schwarz, E. J., Clark, K. R., and Fujiwara, Y., 1982, Paleomagnetism of the Sutton Lake Proterozoic inlier,
903 Ontario, Canada: Canadian Journal of Earth Sciences, v. 19, p. 1330–1332, doi:10.1139/e82-114.
- 904 Selkin, P. A., Gee, J. S., Meurer, W. P., and Hemming, S. R., 2008, Paleointensity record from the 2.7 Ga Stillwater
905 Complex, Montana: Geochem. Geophys. Geosyst., v. 9, p. 10.1029/2008GC001,950.
- 906 Silver, P. G. and Behn, M. D., 2008, Intermittent plate tectonics?: Science, v. 319, p. 85–88.
- 907 Skipton, D. R., St-Onge, M. R., Schneider, D. A., and McFarlane, C. R. M., 2016, Tectonothermal evolution of the
908 middle crust in the Trans-Hudson Orogen, Baffin Island, Canada: Evidence from petrology and monazite
909 geochronology of sillimanite-bearing migmatites: Journal of Petrology, v. 57, p. 1437–1462,
910 doi:10.1093/petrology/egw046.
- 911 Slagstad, T., Culshaw, N. G., Daly, J. S., and Jamieson, R. A., 2009, Western Grenville Province holds key to
912 midcontinental Granite-Rhyolite Province enigma: Terra Nova, v. 21, p. 181–187,
913 doi:10.1111/j.1365-3121.2009.00871.x.
- 914 St-Onge, M. R., Van Gool, J. A. M., Garde, A. A., and Scott, D. J., 2009, Correlation of Archaean and
915 Palaeoproterozoic units between northeastern Canada and western Greenland: constraining the pre-collisional
916 upper plate accretionary history of the Trans-Hudson orogen: Geological Society, London, Special Publications,
917 v. 318, p. 193–235, doi:10.1144/sp318.7.
- 918 Stern, R. J. and Miller, N. R., 2018, Did the transition to plate tectonics cause neoproterozoic snowball earth?:
919 Terra Nova, v. 30, p. 87–94, doi:10.1111/ter.12321.
- 920 Stern, R. J., Tsujimori, T., Harlow, G., and Groat, L. A., 2013, Plate tectonic gemstones: Geology, v. 41, p.
921 723–726, doi:10.1130/g34204.1.

- 922 Swanson-Hysell, N. L., Burgess, S. D., Maloof, A. C., and Bowring, S. A., 2014a, Magmatic activity and plate
923 motion during the latent stage of Midcontinent Rift development: *Geology*, v. 42, p. 475–478,
924 doi:10.1130/G35271.1.
- 925 Swanson-Hysell, N. L., Ramezani, J., Fairchild, L. M., and Rose, I. R., 2019, Failed rifting and fast drifting:
926 Midcontinent Rift development, Laurentia's rapid motion and the driver of Grenvillian orogenesis: *GSA Bulletin*,
927 doi:10.1130/b31944.1.
- 928 Swanson-Hysell, N. L., Vaughan, A. A., Mustain, M. R., and Asp, K. E., 2014b, Confirmation of progressive plate
929 motion during the Midcontinent Rift's early magmatic stage from the Osler Volcanic Group, Ontario, Canada:
930 *Geochemistry Geophysics Geosystems*, v. 15, p. 2039–2047, doi:10.1002/2013GC005180.
- 931 Symons, D. and Chiasson, A., 1991, Paleomagnetism of the Callander Complex and the Cambrian apparent polar
932 wander path for North America: *Canadian Journal of Earth Science*, v. 1991, p. 355–363, doi:10.1139/e91-032.
- 933 Symons, D., Symons, T., and Lewchuk, M., 2000, Paleomagnetism of the Deschambault pegmatites: Stillstand and
934 hairpin at the end of the Paleoproterozoic Trans-Hudson Orogeny, Canada: *Physics and Chemistry of the Earth*,
935 Part A: Solid Earth and Geodesy, v. 25, p. 479–487, doi:10.1016/s1464-1895(00)00074-0.
- 936 Symons, D. T. A. and Mackay, C. D., 1999, Paleomagnetism of the Boot-Phantom pluton and the amalgamation of
937 the juvenile domains in the Paleoproterozoic Trans-Hudson Orogen, Canada: *In* Sinha, A. K., ed., *Basement*
938 *Tectonics* 13, Springer Netherlands, Dordrecht, p. 313–331, doi:10.1007/978-94-011-4800-9{_\}18.
- 939 Tanczyk, E., Lapointe, P., Morris, W., and Schmidt, P., 1987, A paleomagnetic study of the layered mafic intrusions
940 at Sept-Iles, Quebec: *Canadian Journal of Earth Science*, v. 24, p. 1431–1438, doi:10.1139/e87-135.
- 941 Tauxe, L. and Kodama, K., 2009, Paleosecular variation models for ancient times: Clues from Keweenawan lava
942 flows: *Physics of the Earth and Planetary Interiors*, v. 177, p. 31–45, doi:10.1016/j.pepi.2009.07.006.
- 943 Tauxe, L., Shaar, R., Jonestrask, L., Swanson-Hysell, N., Minnett, R., Koppers, A., Constable, C., Jarboe, N.,
944 Gaastra, K., and Fairchild, L., 2016, PmagPy: Software package for paleomagnetic data analysis and a bridge to
945 the Magnetics Information Consortium (MagIC) Database: *Geochemistry, Geophysics, Geosystems*,
946 doi:10.1002/2016GC006307.
- 947 Torsvik, T. H. and Cocks, L. R. M., 2017, Earth history and palaeogeography: Cambridge University Press,
948 doi:10.1017/9781316225523.
- 949 Torsvik, T. H., van der Voo, R., Doubrovine, P. V., Burke, K., Steinberger, B., Ashwal, L. D., Trønnes, R. G.,
950 Webb, S. J., and Bull, A. L., 2014, Deep mantle structure as a reference frame for movements in and on the
951 Earth: *Proceedings of the National Academy of Sciences*, doi:10.1073/pnas.1318135111.

- 952 Torsvik, T. H., Van der Voo, R., Preeden, U., Mac Niocaill, C., Steinberger, B., Doubrovine, P. V., van Hinsbergen,
953 D. J. J., Domeier, M., Gaina, C., Tohver, E., Meert, J. G., McCausland, P. J. A., and Cocks, L. R. M., 2012,
954 Phanerozoic polar wander, palaeogeography and dynamics: *Earth-Science Reviews*, v. 114, p. 325–368,
955 doi:10.1016/j.earscirev.2012.06.007.
- 956 Veikkolainen, T., Pesonen, L., and Evans, D. A. D., 2014, PALEOMAGIA: A PHP/MYSQL database of the
957 Precambrian paleomagnetic data: *Studia Geophysica et Geodaetica*, p. 1–17, doi:10.1007/s11200-013-0382-0.
- 958 Warnock, A., Kodama, K., and Zeitler, P., 2000, Using thermochronometry and low-temperature demagnetization
959 to accurately date Precambrian paleomagnetic poles: *Journal of Geophysical Research*, v. 105, p. 19,435–19,453,
960 doi:10.1029/2000jb900114.
- 961 Weil, A., Geissman, J., Heizler, M., and Van der Voo, R., 2003, Paleomagnetism of Middle Proterozoic mafic
962 intrusions and Upper Proterozoic (Nankoweap) red beds from the Lower Grand Canyon Supergroup, Arizona:
963 *Tectonophysics*, v. 375, p. 199–220, doi:10.1016/S0040-1951(03)00339-1.
- 964 Weil, A. B., Geissman, J. W., and Ashby, J. M., 2006, A new paleomagnetic pole for the Neoproterozoic Uinta
965 Mountain supergroup, Central Rocky Mountain States, USA: *Precambrian Research*, v. 147, p. 234–259,
966 doi:10.1016/j.precamres.2006.01.017.
- 967 Weil, A. B., Geissman, J. W., and Voo, R. V. d., 2004, Paleomagnetism of the Neoproterozoic Chuar Group, Grand
968 Canyon Supergroup, Arizona: implications for Laurentia's Neoproterozoic APWP and Rodinia break-up:
969 *Precambrian Research*, v. 129, p. 71–92.
- 970 Weller, O. M. and St-Onge, M. R., 2017, Record of modern-style plate tectonics in the Palaeoproterozoic
971 Trans-Hudson orogen: *Nature Geoscience*, v. 10, doi:10.1038/ngeo2904.
- 972 Whitmeyer, S. and Karlstrom, K., 2007, Tectonic model for the Proterozoic growth of North America: *Geosphere*,
973 v. 3, p. 220–259, doi:10.1130/GES00055.1.
- 974 Witkosky, R. and Wernicke, B. P., 2018, Subsidence history of the Ediacaran Johnnie Formation and related strata
975 of southwest Laurentia: Implications for the age and duration of the Shuram isotopic excursion and animal
976 evolution: *Geosphere*, v. 14, p. 2245–2276, doi:10.1130/ges01678.1.
- 977 Zhang, S., Li, Z.-X., Evans, D. A. D., Wu, H., Li, H., and Dong, J., 2012, Pre-Rodinia supercontinent Nuna shaping
978 up: A global synthesis with new paleomagnetic results from North China: *Earth and Planetary Science Letters*,
979 v. 353–354, p. 145–155.

Table 1. Rotations of separated terranes

Block	Euler pole longitude	Euler pole latitude	rotation angle	note and citation
Greenland	-118.5	67.5	-13.8	Cenozoic separation of Greenland from Laurentia associated with opening of Baffin Bay and the Labrador Sea (Roest and Srivastava, 1989)
Scotland	161.9	78.6	-31.0	Reconstructing Atlantic opening following Torsvik and Cocks (2017)
Svalbard	125.0	-81.0	68	Rotate Svalbard to Laurentia in fit that works well with East Greenland basin according to Maloof et al. (2006)

Table 2: Compilation of paleomagnetic poles from Laurentia

terrane	unit name	Nordic rating	site lon (°)	site lat (°)	plon (°)	plat (°)	A ₉₅ (°)	age (Ma)	pole reference
Laurentia-Wyoming	Stillwater Complex - C2	A	249.2	45.2	335.8	-83.6	4.0	2705 ⁺⁴ ₋₄	Selkin et al. (2008)
Laurentia-Superior(East)	Otto Stock dykes and aureole	B	279.9	48.0	227.0	69.0	4.8	2676 ⁺⁵ ₋₅	Pullaiah and Irving (1975)
Laurentia-Slave	Defeat Suite	B	245.5	62.5	64.0	-1.0	15.0	2625 ⁺⁵ ₋₅	Mitchell et al. (2014)
Laurentia-Superior(East)	Ptarmigan-Mistassini dykes	B	287.0	54.0	213.0	-45.3	13.8	2505 ⁺² ₋₂	Evans and Halls (2010)
Laurentia-Superior(East)	Matachewan dykes	A	278.0	48.0	238.3	-44.1	1.6	2466 ⁺²³ ₋₂₃	Evans and Halls (2010)
Laurentia-Superior(East)	R								
Laurentia-Superior(East)	Matachewan dykes	A	278.0	48.0	239.5	-52.3	2.4	2446 ⁺³ ₋₃	Evans and Halls (2010)
Laurentia-Slave	Malley dykes	A	249.8	64.2	310.0	-50.8	6.7	2231 ⁺² ₋₂	Buchan et al. (2012)
Laurentia-Superior(East)	Senneterre dykes	A	283.0	49.0	284.3	-15.3	5.5	2218 ⁺⁶ ₋₆	Buchan et al. (1993)
Laurentia-Superior(East)	Nipissing N1 sills	A	279.0	47.0	272.0	-17.0	10.0	2217 ⁺⁴ ₋₄	Buchan et al. (2000)
Laurentia-Slave	Dogrib dykes	A	245.5	62.5	315.0	-31.0	7.0	2193 ⁺² ₋₂	Mitchell et al. (2014)
Laurentia-Superior(East)	Biscotasing dykes	A	280.0	48.0	223.9	26.0	7.0	2170 ⁺³ ₋₃	Evans and Halls (2010)
Laurentia-Wyoming	Rabbit Creek, Powder River and South Path Dykes	A	252.8	43.9	339.2	65.5	7.6	2160 ⁺¹¹ ₋₈	Kilian et al. (2015)
Laurentia-Slave	Indin dykes	A	245.6	62.5	256.0	-36.0	7.0	2126 ⁺³ ₋₁₈	Buchan et al. (2016)
Laurentia-Superior(West)	Marathon dykes N	A	275.0	49.0	198.2	45.4	7.7	2124 ⁺³ ₋₃	Halls et al. (2008)

Continued on next page

terrane	unit name	Nordic rating	site lon (°)	site lat (°)	plon (°)	plat (°)	A ₉₅ (°)	age (Ma)	pole reference
Laurentia-Superior(West)	Marathon dykes R	A	275.0	49.0	182.2	55.1	7.5	2104 ₋₃ ⁺³	Halls et al. (2008)
Laurentia-Superior(West)	Cauchon Lake dykes	A	263.0	56.0	180.9	53.8	7.7	2091 ₋₂ ⁺²	Evans and Halls (2010)
Laurentia-Superior(West)	Fort Frances dykes	A	266.0	48.0	184.6	42.8	6.1	2077 ₋₅ ⁺⁵	Evans and Halls (2010)
Laurentia-Superior(East)	Lac Esprit dykes	A	282.0	53.0	170.5	62.0	6.4	2069 ₋₁ ⁺¹	Evans and Halls (2010)
Laurentia-Greenland-Nain	Kangamiut Dykes	B	307.0	66.0	273.8	17.1	2.7	2042 ₋₁₂ ⁺¹²	Fahrig and Bridgwater (1976)
Laurentia-Slave	Lac de Gras dykes	A	249.6	64.4	267.9	11.8	7.1	2026 ₋₅ ⁺⁵	Buchan et al. (2009)
Laurentia-Superior(East)	Minto dykes	A	285.0	57.0	171.5	38.7	13.1	1998 ₋₂ ⁺²	Evans and Halls (2010)
Laurentia-Slave	Rifle Formation	B	252.9	65.9	341.0	14.0	7.7	1963 ₋₆ ⁺⁶	Evans and Hoye (1981)
Laurentia-Rae	Clearwater Anorthosite	B	251.6	57.1	311.8	6.5	2.9	1917 ₋₇ ⁺⁷	Halls and Hanes (1999)
Laurentia-Wyoming	Sourdough mafic dike swarm	A	-108.3	44.7	292.0	49.2	8.1	1899 ₋₅ ⁺⁵	Kilian et al. (2016)
Laurentia-Slave	Ghost Dike Swarm	A	244.6	62.6	286.0	-2.0	6.0	1887 ₋₉ ⁺⁵	Buchan et al. (2016)
Laurentia-Slave	Mean Se-ton/Akaitcho/Mara	B	250.0	65.0	260.0	-6.0	4.0	1885 ₋₅ ⁺⁵	Mitchell et al. (2010)
Laurentia-Slave	Mean Kahochella, Peacock Hills	B	250.0	65.0	285.0	-12.0	7.0	1882 ₋₄ ⁺⁴	Mitchell et al. (2010)
Laurentia-Superior(West)	Molson (B+C2) dykes	A	262.0	55.0	218.0	28.9	3.8	1879 ₋₆ ⁺⁶	Evans and Halls (2010)

Continued on next page

terrane	unit name	Nordic rating	site lon (°)	site lat (°)	plon (°)	plat (°)	A ₉₅ (°)	age (Ma)	pole reference
Laurentia-Slave	Douglas Peninsula Formation, Pethei Group	B	249.7	62.8	258.0	-18.0	14.2	1876 ⁺¹⁰ ₋₁₀	Irving and McGlynn (1979)
Laurentia-Slave	Takiyuak Formation	B	246.9	66.1	249.0	-13.0	8.0	1876 ⁺¹⁰ ₋₁₀	Irving and McGlynn (1979)
Laurentia-Superior	Haig/Flaherty/Sutton Mean	B	279.0	56.0	245.8	1.0	3.9	1870 ⁺¹ ₋₁	Nordic workshop calculation based on data of Schmidt (1980); Schwarz et al. (1982)
Laurentia-Slave	Pearson A/Peninsular/Kilohigok sills	A	250.0	65.0	269.0	-22.0	6.0	1870 ⁺⁴ ₋₄	Mitchell et al. (2010)
Laurentia-Trans-Hudson orogen	Boot-Phantom Pluton	B	258.1	54.7	275.4	62.4	7.9	1838 ⁺¹ ₋₁	Symons and Mackay (1999)
Laurentia-Rae	Sparrow Dykes	B	250.2	61.6	291.0	12.0	7.9	1827 ⁺⁴ ₋₄	McGlynn et al. (1974)
Laurentia-Rae	Martin Formation	A	251.4	59.6	288.0	-9.0	8.5	1818 ⁺⁴ ₋₄	Evans and Bingham (1973)
Laurentia	Dubawnt Group	B	265.6	64.1	277.0	7.0	8.0	1785 ⁺³⁵ ₋₃₅	Park et al. (1973)
Laurentia-Trans-Hudson orogen	Deschambault Pegmatites	B	256.7	54.9	276.0	67.5	7.7	1766 ⁺⁵ ₋₅	Symons et al. (2000)
Laurentia-Trans-Hudson orogen	Jan Lake Granite	B	257.2	54.9	264.3	24.3	16.9	1758 ⁺¹ ₋₁	Gala et al. (1995)
Laurentia	Cleaver Dykes	A	242.0	67.5	276.7	19.4	6.1	1741 ⁺⁵ ₋₅	Irving (2004)
Laurentia-Greenland	Melville Bugt dia-base dykes	B	303.0	74.6	273.8	5.0	8.7	1633 ⁺⁵ ₋₅	Halls et al. (2011)
Laurentia	Western Channel Diabase	A	242.2	66.4	245.0	9.0	6.6	1590 ⁺³ ₋₃	Irving and Park (1972)

Continued on next page

terrane	unit name	Nordic rating	site lon (°)	site lat (°)	plon (°)	plat (°)	A ₉₅ (°)	age (Ma)	pole reference
Laurentia	St.Francois Mountains Acidic Rocks	A	269.5	37.5	219.0	-13.2	6.1	1476 ⁺¹⁶ ₋₁₆	Meert and Stuckey (2002)
Laurentia	Michikamau Intrusion	A	296.0	54.5	217.5	-1.5	4.7	1460 ⁺⁵ ₋₅	Emslie et al. (1976)
Laurentia	Spokane Formation	A	246.8	48.2	215.5	-24.8	4.7	1458 ⁺¹³ ₋₁₃	Elston et al. (2002)
Laurentia	Snowslip Formation	A	245.9	47.9	210.2	-24.9	3.5	1450 ⁺¹⁴ ₋₁₄	Elston et al. (2002)
Laurentia	Tobacco Root dykes	B	247.6	47.4	216.1	8.7	10.5	1448 ⁺⁴⁹ ₋₄₉	Harlan et al. (2008)
Laurentia	Purcell Lava	A	245.1	49.4	215.6	-23.6	4.8	1443 ⁺⁷ ₋₇	Elston et al. (2002)
Laurentia	Rocky Mountain intrusions	B	253.8	40.3	217.4	-11.9	9.7	1430 ⁺¹⁵ ₋₁₅	Nordic workshop calculation based on data of Harlan et al. (1994); Harlan and Geissman (1998)
Laurentia	Mistastin Pluton	B	296.3	55.6	201.5	-1.0	7.6	1425 ⁺²⁵ ₋₂₅	Fahrig and Jones (1976)
Laurentia	McNamara Formation	A	246.4	46.9	208.3	-13.5	6.7	1401 ⁺⁶ ₋₆	Elston et al. (2002)
Laurentia	Pilcher, Garnet Range and Libby Formations	A	246.4	46.7	215.3	-19.2	7.7	1385 ⁺²³ ₋₂₃	Elston et al. (2002)
Laurentia-Greenland	Zig-Zag Dal Basalts	B	334.8	81.2	242.8	12.0	3.8	1382 ⁺² ₋₂	Marcussen and Abrahamsen (1983)
Laurentia-Greenland	Midsommersoe Dolerite	B	333.4	81.6	242.0	6.9	5.1	1382 ⁺² ₋₂	Marcussen and Abrahamsen (1983)
Laurentia-Greenland	Victoria Fjord dolerite dykes	B	315.3	81.5	231.7	10.3	4.3	1382 ⁺² ₋₂	Abrahamsen and Van Der Voo (1987)

Continued on next page

terrane	unit name	Nordic rating	site lon (°)	site lat (°)	plon (°)	plat (°)	A ₉₅ (°)	age (Ma)	pole reference
Laurentia	Nain Anorthosite	B	298.2	56.5	206.7	11.7	2.2	1305 ⁺¹⁵ ₋₁₅	Murthy (1978)
Laurentia-Greenland	North Qoroq intrusives	B	314.6	61.1	202.6	13.2	8.3	1275 ⁺¹ ₋₁	Piper (1992)
Laurentia-Greenland	Kungnat Ring Dyke	B	311.7	61.2	198.7	3.4	3.2	1275 ⁺² ₋₂	Piper and Stearn (1977)
Laurentia	Mackenzie dykes	A	250.0	65.0	190.0	4.0	5.0	1267 ⁺² ₋₂	Buchan et al. (2000)
	grand mean								
Laurentia-Greenland	West Gardar Dolerite Dykes	B	311.7	61.2	201.7	8.7	6.6	1244 ⁺⁸ ₋₈	Piper and Stearn (1977)
Laurentia-Greenland	West Gardar Lamprophyre Dykes	B	311.7	61.2	206.4	3.2	7.2	1238 ⁺¹¹ ₋₁₁	Piper and Stearn (1977)
Laurentia	Sudbury Dykes	A	278.6	46.3	192.8	-2.5	2.5	1237 ⁺⁵ ₋₅	Palmer et al. (1977)
	Combined								
Laurentia-Scotland	Stoer Group	B	354.5	58.0	238.4	37.2	7.7	1199 ⁺⁷⁰ ₋₇₀	Nordic workshop calculation
Laurentia-Greenland	Narssaq Gabbro	B	313.8	60.9	225.4	31.6	9.7	1184 ⁺⁵ ₋₅	Piper (1977)
Laurentia-Greenland	Hviddal Giant Dyke	B	313.7	60.9	215.3	33.2	9.6	1184 ⁺⁵ ₋₅	Piper (1977)
Laurentia-Greenland	South Qoroq Intr.	A	314.6	61.1	215.9	41.8	13.1	1163 ⁺² ₋₂	Piper (1992)
Laurentia-Greenland	Giant Gabbro Dykes	B	313.7	60.9	226.1	42.3	9.4	1163 ⁺² ₋₂	Piper (1977)
Laurentia-Greenland	NE-SW Trending dykes	B	314.6	61.1	230.8	33.4	5.7	1160 ⁺⁵ ₋₅	Piper (1992)
Laurentia	Ontario lamprophyre dykes	NR	273.3	48.8	223.3	58.0	9.2	1143 ⁺¹⁰ ₋₁₀	Piispa et al. (2018)

Continued on next page

terrane	unit name	Nordic rating	site lon (°)	site lat (°)	plon (°)	plat (°)	A ₉₅ (°)	age (Ma)	pole reference
Laurentia	Abitibi Dykes	A	279.0	48.0	215.5	48.8	14.1	1141 ₋₂ ⁺²	Ernst and Buchan (1993)
Laurentia	Nipigon sills and lavas	A	270.9	49.1	217.8	47.2	4.0	1109 ₋₂ ⁺²	Nordic workshop calculation based on data of Palmer (1970); Robertson and Fahrig (1971); Pesonen (1979); Pesonen and Halls (1979); Middleton et al. (2004); Borradaile and Middleton (2006)
Laurentia	Lowermost Mamainse Point volcanics -R1	A	275.3	47.1	227.0	49.5	5.3	1109 ₋₃ ⁺²	Swanson-Hysell et al. (2014a)
Laurentia	Lower Osler volcanics -R	A	272.3	48.8	218.6	40.9	4.8	1108 ₋₃ ⁺³	Swanson-Hysell et al. (2014b)
Laurentia	Middle Osler volcanics -R	A	272.4	48.8	211.3	42.7	8.2	1107 ₋₄ ⁺⁴	Swanson-Hysell et al. (2014b)
Laurentia	Upper Osler volcanics -R	A	272.4	48.7	203.4	42.3	3.7	1105 ₋₁ ⁺¹	Halls (1974); Swanson-Hysell et al. (2014b, 2019)
Laurentia	Lower Mamainse Point volcanics -R2	A	275.3	47.1	205.2	37.5	4.5	1105 ₋₄ ⁺³	Swanson-Hysell et al. (2014a)
Laurentia	Mamainse Point volcanics -C (lower N, upper R)	A	275.3	47.1	189.7	36.1	4.9	1101 ₋₁ ⁺¹	Swanson-Hysell et al. (2014a)
Laurentia	North Shore lavas -N	A	268.7	46.3	181.7	31.1	2.1	1097 ₋₃ ⁺³	Tauxe and Kodama (2009); Swanson-Hysell et al. (2019)

Continued on next page

terrane	unit name	Nordic rating	site lon (°)	site lat (°)	plon (°)	plat (°)	A ₉₅ (°)	age (Ma)	pole reference
Laurentia	Portage Lake Volcanics	A	271.2	47.0	182.5	27.5	2.3	1095 ₋₃ ⁺³	Books (1972); Hnat et al. (2006) as calculated in Swanson-Hysell et al. (2019)
Laurentia	Chengwatana Volcanics	B	267.3	45.4	186.1	30.9	8.2	1095 ₋₂ ⁺²	Kean et al. (1997)
Laurentia	Uppermost Mainse Point volcanics -N	A	275.3	47.1	183.2	31.2	2.5	1094 ₋₄ ⁺⁶	Swanson-Hysell et al. (2014a)
Laurentia	Cardenas Basalts and Intrusions	B	248.1	36.1	185.0	32.0	8.0	1091 ₋₅ ⁺⁵	Weil et al. (2003)
Laurentia	Schroeder Lutsen Basalts	A	269.1	47.5	187.8	27.1	3.0	1090 ₋₇ ⁺²	Fairchild et al. (2017)
Laurentia	Central Arizona diabases -N	A	249.2	33.7	175.3	15.7	7.0	1088 ₋₁₁ ⁺¹¹	Donadini et al. (2011)
Laurentia	Lake Shore Traps	A	271.9	47.6	186.4	23.1	4.0	1086 ₋₁ ⁺¹	Kulakov et al. (2013)
Laurentia	Michipicoten Island Formation	A	274.3	47.7	174.7	17.0	4.4	1084 ₋₁ ⁺¹	Fairchild et al. (2017)
Laurentia	Nonesuch Shale	B	271.5	47.0	178.1	7.6	5.5	1080 ₋₁₀ ⁺⁴	Henry et al. (1977)
Laurentia	Freda Sandstone	B	271.5	47.0	179.0	2.2	4.2	1070 ₋₁₀ ⁺¹⁴	Henry et al. (1977)
Laurentia	Haliburton Intrusions	B	281.4	45.0	141.9	-32.6	6.3	1015 ₋₁₅ ⁺¹⁵	Warnock et al. (2000)
Laurentia-Scotland	Torridon Group	B	354.3	57.9	220.9	-17.7	7.1	925 ₋₁₄₅ ⁺¹⁴⁵	Nordic workshop calculation
Laurentia-Svalbard	Lower Grusdievbreen Formation	B	18.0	79.0	204.9	19.6	10.9	831 ₋₂₀ ⁺²⁰	Maloof et al. (2006)

Continued on next page

terrane	unit name	Nordic rating	site lon (°)	site lat (°)	plon (°)	plat (°)	A ₉₅ (°)	age (Ma)	pole reference
Laurentia-Svalbard	Upper Grus-dievbreen Formation	B	18.2	78.9	252.6	-1.1	6.2	800 ⁺¹¹ ₋₁₁	Maloof et al. (2006)
Laurentia	Gunbarrel dykes	B	248.7	44.8	138.2	9.1	12.0	778 ⁺² ₋₂	Calculation from Eyster et al. (2019) based on data of Harlan (1993); Harlan et al. (1997)
Laurentia-Svalbard	Svanbergfjellet Formation	B	18.0	78.5	226.8	25.9	5.8	770 ⁺¹⁹ ₋₄₀	Maloof et al. (2006)
Laurentia	Uinta Mountain Group	B	250.7	40.8	161.3	0.8	4.7	760 ⁺⁶ ₋₁₀	Weil et al. (2006)
Laurentia	Carbon Canyon	NR	248.2	36.1	166.0	-0.5	9.7	757 ⁺⁷ ₋₇	Weil et al. (2004) as calculated in Eyster et al. (2019)
Laurentia	Carbon Butte/Awatubi	NR	248.5	35.2	163.8	14.2	3.5	751 ⁺⁸ ₋₈	Eyster et al. (2019)
Laurentia	Franklin event grand mean	A	275.4	73.0	162.1	6.7	3.0	724 ⁺³ ₋₃	Denyszyn et al. (2009a)
Laurentia	Long Range Dykes	B	303.3	53.7	355.3	19.0	17.4	615 ⁺² ₋₂	Murthy et al. (1992)
Laurentia	Baie des Moutons complex	B	301.0	50.8	321.5	-34.2	15.4	583 ⁺² ₋₂	McCausland et al. (2011)
Laurentia	Baie des Moutons complex	B	301.0	50.8	332.7	42.6	12.0	583 ⁺² ₋₂	McCausland et al. (2011)
Laurentia	Callander Alkaline Complex	B	280.6	46.2	301.4	46.3	6.0	575 ⁺⁵ ₋₅	Symons and Chiasson (1991)
Laurentia	Catoctin Basalts	B	281.8	38.5	296.7	42.0	17.5	572 ⁺⁵ ₋₅	Meert et al. (1994)

Continued on next page

terrane	unit name	Nordic rating	site lon (°)	site lat (°)	plon (°)	plat (°)	A ₉₅ (°)	age (Ma)	pole reference
Laurentia	Sept-Iles layered intrusion	B	293.5	50.2	321.0	-20.0	6.7	565 ⁺⁴ ₋₄	Tanczyk et al. (1987)